5. INTEGRATED MAGNETICS

Parts of this chapter have been published in IEEE Power Electronic Letters in 2005 and in the Proceedings of AUPEC 2005.

The two-inductor boost converter has been proven to be favourable in the applications where low-voltage high-current dc input needs to be transformed to high-voltage dc output. The high dc voltage gain, the low switch voltage stress, the full utilisation of the transformer windings, the ease in the transformer volt-second balance and the relaxed diode reverse recovery requirement are several advantages of this boost-derived converter. In the effort of reducing the converter size by increasing the switching frequency, the soft-switching technique is employed and the ZVS two-inductor boost converter results as shown in Chapter 4. In both the hard-switched and the soft-switched forms, however, the two-inductor boost converter requires at least three separate magnetic components including two inductors and one transformer, which are accounted for the bulk, weight and cost [150]. This requirement also departs from the philosophy of "more silicon and less iron" in the design of the modern power electronic converters [91]. If three separate magnetic components can be merged into a single magnetic structure, not only can the size of the converter be greatly reduced, but also the converter will be more cost effective.

The magnetic core integration theory was formally presented more than twenty years

ago as a way to assist in reducing the size of the switch mode power converters [151]-[153], while a simple showcase of the application can be traced back to early 1930's [154]. Recently, winding integration concept has been proposed as a new technique in reducing the winding cost and improving the efficiency [155]. Over the years, these integrated magnetic approaches have been widely applied to the current-doubler rectifier circuit [138], [142], [143], [156]-[161].

This chapter provides a generic approach to the magnetic integration of the two inductors and the transformer in the two-inductor boost converter and presents a detailed analysis of the individual structures. Four integrated magnetic structures will be discussed in detail which will be referred as Structures A, B, C and D. Structure A is a new structure and has been independently proposed by Gao and Ayyannar in [130] and by the author in [162]. This structure first appears in this thesis in Figure 5.5 on page 170. Structure B is also a new structure and has been proposed by the author in [163]. This structure first appears in this thesis in Figure 5.9 on page 189. Structure C has been proposed by Gao and Ayyannar in [130] and by Yan and Lehman in [144] and [145]. This structure first appears in this thesis in Figure 5.11 on page 192. Structure D has been independently proposed by Gao and Ayyannar in [130], by Yan and Lehman in [145] and by the author in [164] while a major contribution of this thesis is a comprehensive analysis of the structure. This structure first appears in this thesis in Figure 5.13 on page 198.

The equivalent input and magnetising inductance values of the two-inductor boost converter with integrated magnetics are established and the comparisons of the four

different magnetic structures are provided. A soft-switched two-inductor boost converter with Structure B magnetic integration is also analysed in detail.

5.1 State Analysis of the Hard-Switched Two-Inductor Boost Converter with Discrete Magnetics

In order to analyse the two-inductor boost converter with the integrated magnetic structures, state analysis must be first conducted for the converter with discrete magnetic components. Figure 5.1 shows the hard-switched two-inductor boost converter with a voltage-doubler rectifier. In the analysis, all the components are considered to be ideal and the capacitors in the voltage-doubler rectifier are assumed to be large enough so that the output is a pure dc voltage.

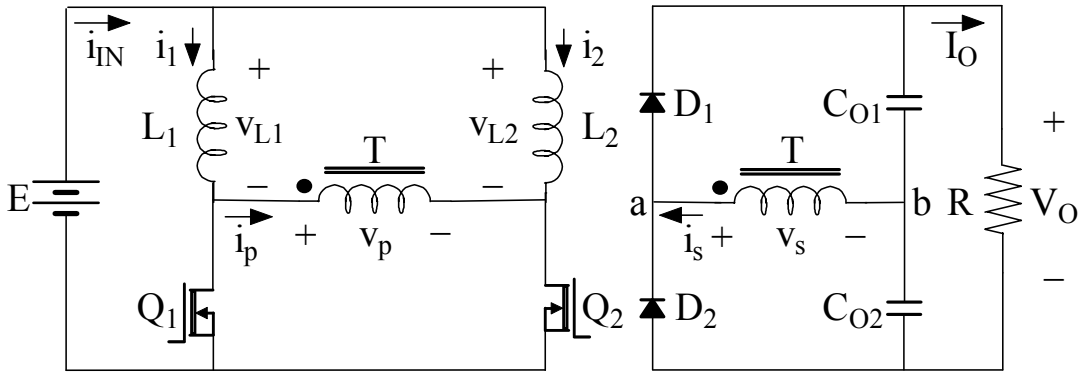

Figure 5.1 Hard-Switched Two-Inductor Boost Converter

Before Q_1 turns off, both Q_1 and Q_2 are on. At time $t = 0$, Q_1 turns off and the converter will move through four states within a switching period as shown in Figure 5.2. In order to be different from the state analysis in the ZVS two-inductor

boost converter, where States (a) to (d) are used for the individual resonant states over a half switching period, States (1) to (4) are used here for the individual switching states over one complete switching period.

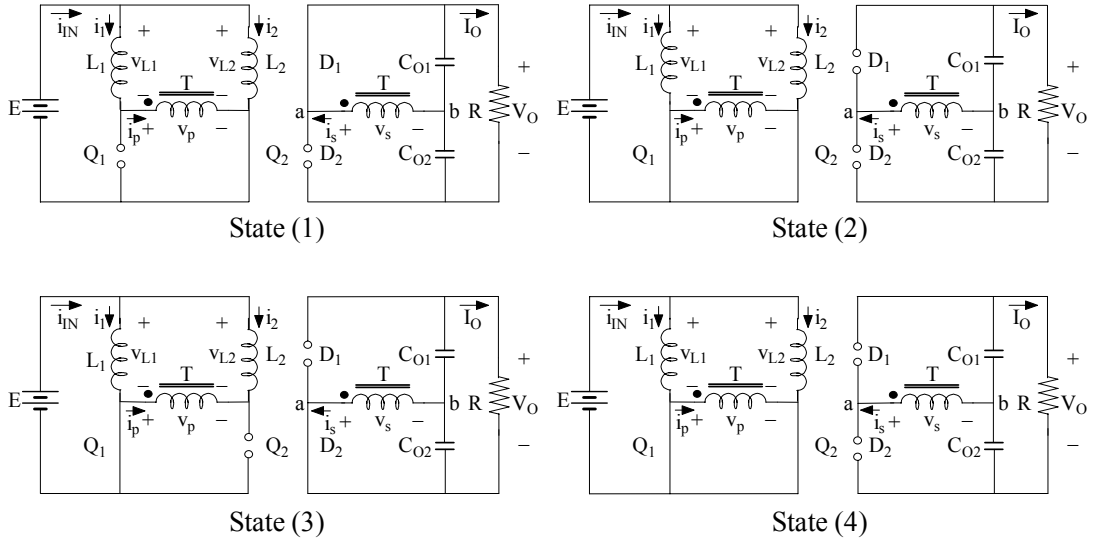

Figure 5.2 Four States of the Hard-Switched Two-Inductor Boost Converter

The duty ratio of the MOSFETs is D_s and it must be greater than 50% to prevent the open circuit of the currents in the two inductors from happening. The switching period is T_s. The input inductance is $L_1 = L_2 = L$. The numbers of turns of the transformer T primary and secondary windings are respectively N_p and N_s. The voltages of the transformer T primary and secondary are respectively v_p and v_s. The transformer magnetising inductance reflected to the secondary side is L_{ms}. In the analysis of each state, the derivatives of the instantaneous converter input current $i_{IN} = i_1 + i_2$ and the instantaneous transformer secondary current i_s are solved. These equations will be used as the templates to obtain the equivalent circuits of the

converter with integrated magnetics later in the chapter.

- State (1) ($0 < t < (1 - D_s)T_s$)

In this state, Q_1 is off and Q_2 is on. The circuit equations are:

$$L\frac{di_1}{dt} = E - v_p \tag{5.1}$$

$$L\frac{di_2}{dt} = E \tag{5.2}$$

$$v_p = \frac{N_p}{N_s} v_s \tag{5.3}$$

Manipulations of Equations (5.1) to (5.3) yield:

$$\frac{d(i_1 + i_2)}{dt} = \frac{1}{L}\left(2E - \frac{N_p}{N_s} v_s\right) \tag{5.4}$$

The transformer model with the magnetising inductance reflected to the secondary side is used to derive $\frac{di_s}{dt}$, as shown in Figure 5.3. The currents in the ideal transformer primary and secondary windings are respectively i_p and i_{s1}, and the transformer magnetising current reflected to the secondary side is i_{s2}.

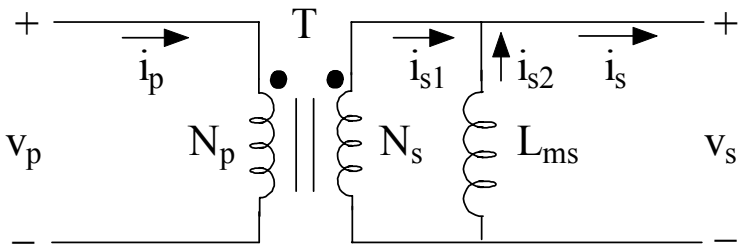

Figure 5.3 Equivalent Transformer Model

The following equations can be obtained from Figures 5.2 and 5.3:

$$i_{s1} = \frac{N_p}{N_s} i_p \tag{5.5}$$

$$i_p = i_1 \tag{5.6}$$

Manipulations of Equations (5.1), (5.3), (5.5) and (5.6) yield:

$$\frac{di_{s1}}{dt} = \frac{N_p}{N_s} \cdot \frac{E}{L} - \left(\frac{N_p}{N_s}\right)^2 \frac{v_s}{L} \tag{5.7}$$

The transformer model in Figure 5.3 also gives:

$$\frac{di_{s2}}{dt} = -\frac{v_s}{L_{ms}} \tag{5.8}$$

$$i_s = i_{s1} + i_{s2} \tag{5.9}$$

Manipulations of Equations (5.7) to (5.9) yield:

$$\frac{di_s}{dt} = \frac{N_p}{N_s} \cdot \frac{E}{L} - \left[\frac{1}{L_{ms}} + \left(\frac{N_p}{N_s} \right)^2 \frac{1}{L} \right] v_s \tag{5.10}$$

- State (2) ($(1 - D_s)T_s < t < \frac{T_s}{2}$)

In this state, Q_1 and Q_2 are both on. Following the process in State (a), the derivative of the input current can be found as:

$$\frac{d(i_1 + i_2)}{dt} = \frac{1}{L} 2E \tag{5.11}$$

According to Figure 5.2, the following equation can be obtained:

$$v_s = 0 \tag{5.12}$$

As the transformer secondary voltage is zero, both of the diodes D_1 and D_2 are reverse biased and the transformer secondary current is zero at all times within this state. The derivative of the input current is:

$$\frac{di_s}{dt} = 0 \tag{5.13}$$

- State (3) $(\frac{T_s}{2} < t < (\frac{3}{2} - D_s)T_s)$

In this state, Q_1 is on and Q_2 is off. The derivatives of the input and the transformer secondary currents are respectively:

$$\frac{d(i_1 + i_2)}{dt} = \frac{1}{L}\left(2E + \frac{N_p}{N_s}v_s\right) \tag{5.14}$$

$$\frac{di_s}{dt} = -\frac{N_p}{N_s}\cdot\frac{E}{L} - \left[\frac{1}{L_{ms}} + \left(\frac{N_p}{N_s}\right)^2\frac{1}{L}\right]v_s \tag{5.15}$$

- State (4) $((\frac{3}{2} - D_s)T_s < t < T_s)$

This state repeats State (2) and the derivatives of the input and the transformer secondary currents are respectively given in Equations (5.11) and (5.13).

The current waveforms in the hard-switched two-inductor boost converter are shown in Figure 5.4.

5.2 Integrated Magnetics with Magnetic Core Integration

A fundamental magnetic integration solution for the two-inductor boost converter is to combine the three individual cores to a single core while still maintaining the four

individual windings including two for the inductors, one for the transformer primary and one for the transformer secondary. This approach is named as Structure A as shown in Figure 5.5 and the analysis is given below.

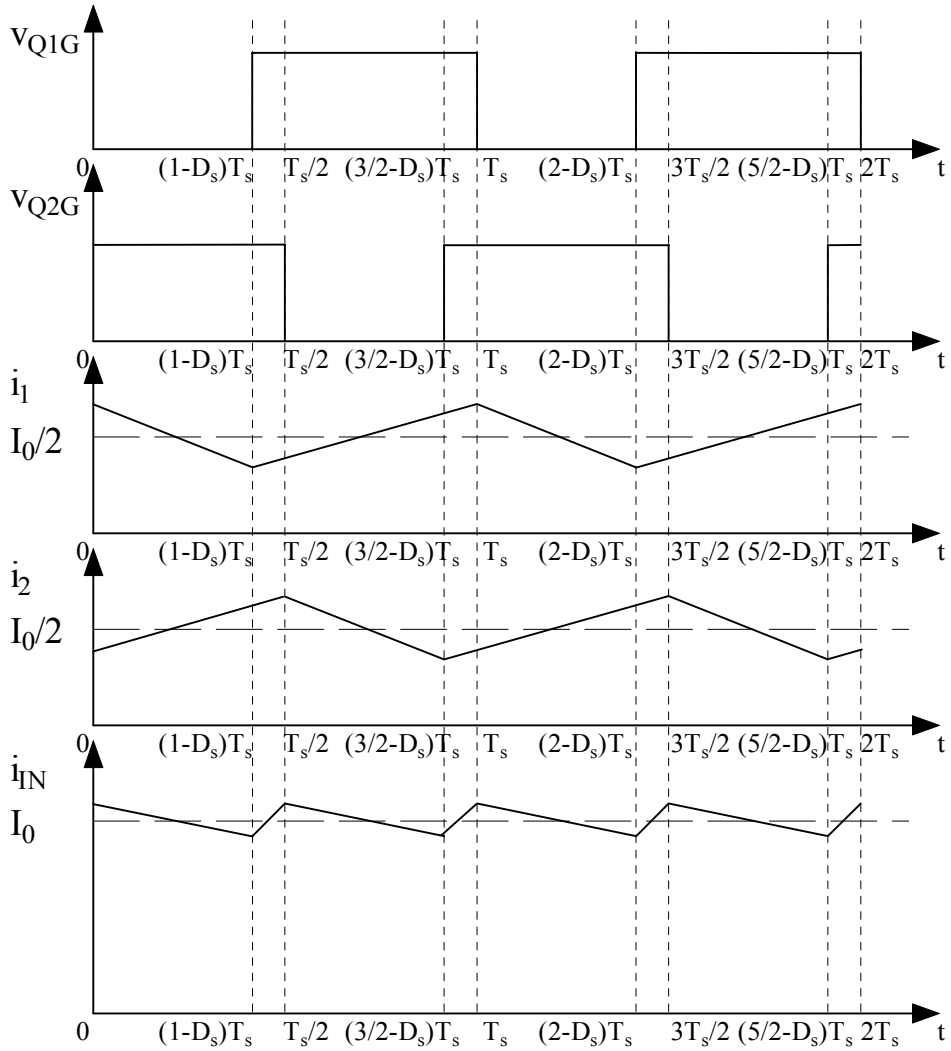

Figure 5.4 Current Waveforms in the Hard-Switched Two-Inductor Boost Converter

5.2.1 Two-Inductor Boost Converter with Structure A Magnetic Integration

The two-inductor boost converter with Structure A magnetic integration is shown in

Figure 5.5.

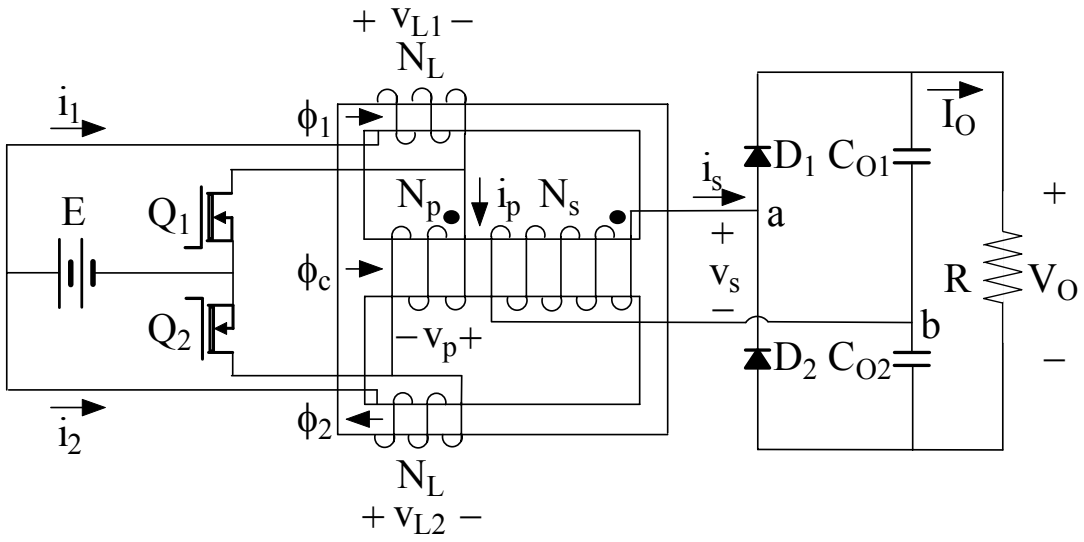

Figure 5.5 Two-Inductor Boost Converter with Structure A Magnetic Integration

The KVL requires that the voltages across the three windings on the converter primary side satisfy the following relationship:

$$v_p = v_{L2} - v_{L1} \tag{5.16}$$

Application of Faraday's Law yields:

$$N_p \frac{d\phi_c}{dt} = N_L \frac{d\phi_2}{dt} - N_L \frac{d\phi_1}{dt} \tag{5.17}$$

where N_L is the number of turns of the two input inductors L_1 and L_2, and ϕ_1, ϕ_2, ϕ_c

are respectively the instantaneous fluxes in the two outer and the centre core legs and they obey the following equation:

$$\phi_c = \phi_2 - \phi_1 \tag{5.18}$$

Manipulations of Equations (5.17) and (5.18) yield:

$$N_p = N_L \tag{5.19}$$

Equation (5.19) is the inherent constraint of Structure A magnetic integration. If this constraint is not fulfilled, the magnetic integration becomes impossible as Equation (5.18) cannot be established in the magnetic core.

5.2.2 Equivalent Input and Transformer Magnetising Inductances

In order to obtain the equivalent input and transformer magnetising inductances of the two-inductor boost converter with Structure A magnetic integration, the converter must be analysed under three different operating conditions.

- State (1) ($v_s > 0$)

  In this state, Q_1 is off while Q_2 is on and i_1 flows in the transformer primary winding. The magnetic circuit is drawn in Figure 5.6(a), where $\Re_o$ and $\Re_c$ are

respectively the reluctances of the outer and the centre core legs. The fluxes in the two outer core legs are respectively:

$$\phi_1 = \frac{N_p i_1}{\Re_o + 2\Re_c} \cdot \frac{\Re_c}{\Re_o} + \frac{N_s i_s}{\Re_o + 2\Re_c} + \frac{N_p i_2}{\Re_o + 2\Re_c} \cdot \frac{\Re_c}{\Re_o} \tag{5.20}$$

$$\phi_2 = \frac{N_p i_1}{\Re_o + 2\Re_c}\left(1 + \frac{\Re_c}{\Re_o}\right) - \frac{N_s i_s}{\Re_o + 2\Re_c} + \frac{N_p i_2}{\Re_o + 2\Re_c}\left(1 + \frac{\Re_c}{\Re_o}\right) \tag{5.21}$$

According to Figure 5.5, Faraday's Law gives:

$$N_p \frac{d\phi_1}{dt} = E - \frac{N_p}{N_s} v_s \tag{5.22}$$

$$N_p \frac{d\phi_2}{dt} = E \tag{5.23}$$

Substitution of Equations (5.20) and (5.21) to (5.22) and (5.23) yields:

$$\frac{d(i_1 + i_2)}{dt} = \frac{\Re_o}{N_p^2}\left(2E - \frac{N_p}{N_s} v_s\right) \tag{5.24}$$

$$\frac{di_s}{dt} = \frac{\Re_o}{N_p N_s} E - \frac{\Re_o + \Re_c}{N_s^2} v_s \tag{5.25}$$

By defining L_a and L_b as:

$$L_a = \frac{N_p^2}{\Re_o} \tag{5.26}$$

$$L_b = \frac{2N_s^2}{\Re_o + 2\Re_c} \tag{5.27}$$

Equations (5.24) and (5.25) can be simplified to:

$$\frac{d(i_1 + i_2)}{dt} = \frac{1}{L_a}\left(2E - \frac{N_p}{N_s} v_s\right) \tag{5.28}$$

$$\frac{di_s}{dt} = \frac{N_p}{N_s} \cdot \frac{E}{L_a} - \left[\frac{1}{L_b} + \left(\frac{N_p}{N_s}\right)^2 \frac{1}{2L_a}\right] v_s \tag{5.29}$$

- State (3) ($v_s < 0$)

In this state, Q_1 is on while Q_2 is off and i_2 flows in the transformer primary winding. The magnetic circuit is drawn in Figure 5.6(b). The fluxes in the two outer core legs are respectively:

$$\phi_1 = \frac{N_p i_1}{\Re_o + 2\Re_c}\left(1 + \frac{\Re_c}{\Re_o}\right) + \frac{N_s i_s}{\Re_o + 2\Re_c} + \frac{N_p i_2}{\Re_o + 2\Re_c}\left(1 + \frac{\Re_c}{\Re_o}\right) \tag{5.30}$$

$$\phi_2 = \frac{N_p i_1}{\Re_o + 2\Re_c} \cdot \frac{\Re_c}{\Re_o} - \frac{N_s i_s}{\Re_o + 2\Re_c} + \frac{N_p i_2}{\Re_o + 2\Re_c} \cdot \frac{\Re_c}{\Re_o} \tag{5.31}$$

According to Figure 5.5, Faraday's Law gives:

$$N_p \frac{d\phi_1}{dt} = E \tag{5.32}$$

$$N_p \frac{d\phi_2}{dt} = E + \frac{N_p}{N_s} v_s \tag{5.33}$$

Substitution of Equations (5.30) and (5.31) to (5.32) and (5.33) yields:

$$\frac{d(i_1 + i_2)}{dt} = \frac{\Re_o}{N_p^2}\left(2E + \frac{N_p}{N_s} v_s\right) \tag{5.34}$$

$$\frac{di_s}{dt} = -\frac{\Re_o}{N_p N_s} E - \frac{\Re_o + \Re_c}{N_s^2} v_s \tag{5.35}$$

Equations (5.34) and (5.35) can be simplified by the definitions of L_a and L_b in Equations (5.26) and (5.27) to:

$$\frac{d(i_1 + i_2)}{dt} = \frac{1}{L_a}\left(2E + \frac{N_p}{N_s} v_s\right) \tag{5.36}$$

$$\frac{di_s}{dt} = -\frac{N_p}{N_s}\frac{E}{L_a} - \left[\frac{1}{L_b} + \left(\frac{N_p}{N_s}\right)^2 \frac{1}{2L_a}\right] v_s \tag{5.37}$$

- States (2) and (4) ($v_s = 0$)

In these two states, Q_1 and Q_2 are both on and the transformer primary current is

zero. The magnetic circuit is drawn in Figure 5.6(c). The fluxes in the two outer core legs are respectively:

$$\phi_1 = \frac{N_p i_1}{\Re_o + 2\Re_c}\left(1 + \frac{\Re_c}{\Re_o}\right) + \frac{N_p i_2}{\Re_o + 2\Re_c} \cdot \frac{\Re_c}{\Re_o} \tag{5.38}$$

$$\phi_2 = \frac{N_p i_1}{\Re_o + 2\Re_c} \cdot \frac{\Re_c}{\Re_o} + \frac{N_p i_2}{\Re_o + 2\Re_c}\left(1 + \frac{\Re_c}{\Re_o}\right) \tag{5.39}$$

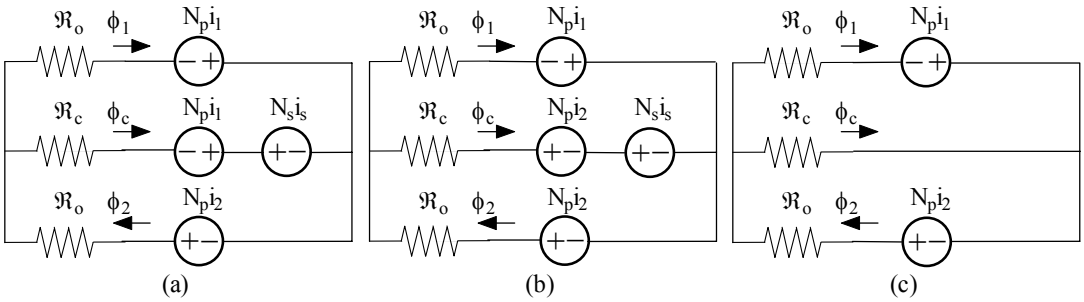

Figure 5.6 Structure A Magnetic Circuits

(a) State (1) (b) State (3) (c) States (2) and (4)

According to Figure 5.5, Faraday's Law gives Equations (5.23), (5.32) and (5.40):

$$N_s \frac{d\phi_c}{dt} = v_s \tag{5.40}$$

Substitution of Equations (5.38) and (5.39) to (5.23) and (5.32) yields:

$$\frac{d(i_1 + i_2)}{dt} = \frac{\Re_o}{N_p^2} 2E \tag{5.41}$$

Equation (5.41) can be simplified by the definition of L_a in Equation (5.26) to:

$$\frac{d(i_1 + i_2)}{dt} = \frac{1}{L_a} 2E \tag{5.42}$$

Manipulations of Equations (5.18), (5.23), (5.32) and (5.40) yield Equation (5.12). Therefore, Equation (5.13) is still valid in this state.

Comparisons of Equations (5.28), (5.29), (5.36), (5.37) and (5.42) respectively with their discrete magnetic counterparts, Equations (5.4), (5.10), (5.14), (5.15) and (5.11), yield:

$$L = L_a = \frac{N_p^2}{\Re_o} \tag{5.43}$$

$$L_{ms} = \frac{1}{\frac{1}{L_b} - \left(\frac{N_p}{N_s}\right)^2 \frac{1}{2L_a}} = \frac{N_s^2}{\Re_c} \tag{5.44}$$

Equations (5.43) and (5.44) imply that other than the number of turns, the input inductances are inversely proportional to the reluctance of the outer core leg and the magnetising inductance is inversely proportional to that of the centre core leg. This normally requires that the outer core legs be gapped to store the energy in the input

inductors and prevent the core from saturation. The gapping of the centre core leg is possible but not indispensable.

5.2.3 DC Gain

As the voltages across the two windings on the outer core legs are finite, the fluxes in the two outer core legs must be continuous. This corresponds to the more familiar statement that the current in the inductor must be continuous in the circumstance with discrete magnetics.

Consider the flux in one outer core leg ϕ_1. According to Figure 5.5, Faraday's Law gives Equation (5.22) in State (1) when Q_1 is off and Equation (5.32) in States (2) to (4) when Q_1 is on. In State (1), the transformer secondary voltage can be found as:

$$v_s = v_{s,1} = \frac{V_O}{2} \tag{5.45}$$

Therefore, Equation (5.22) can be rewritten as:

$$N_p \frac{d\phi_1}{dt} = E - \frac{N_p}{N_s} \cdot \frac{V_O}{2} \tag{5.46}$$

As the derivatives of the flux ϕ_1 in Equations (5.32) and (5.46) are constants, the change of the flux when Q_1 is off, $(\Delta\phi_1)_{Q1,off}$, and that when Q_1 is on, $(\Delta\phi_1)_{Q1,on}$, are respectively:

$$(\Delta\phi_1)_{Q1,off} = \frac{\left(E - \frac{N_p}{N_s}\cdot\frac{V_O}{2}\right)(1-D_s)T_s}{N_p} \tag{5.47}$$

$$(\Delta\phi_1)_{Q1,on} = \frac{ED_sT_s}{N_p} \tag{5.48}$$

Due to the continuity of the flux, the following equation can be obtained:

$$(\Delta\phi_1)_{Q1,off} + (\Delta\phi_1)_{Q1,on} = 0 \tag{5.49}$$

Substitution of Equations (5.47) and (5.48) to (5.49) and solving for V_O yield:

$$V_O = \frac{N_s}{N_p}\cdot\frac{2}{1-D_s}E \tag{5.50}$$

Equation (5.50) validates that the two-inductor boost converter with Structure A magnetic integration has the same dc voltage gain as the converter with discrete magnetics.

5.2.4 DC and AC Flux Densities

In order to prevent the magnetic core from saturation, the peak flux density in each core leg must be established. The ac fluxes must be also investigated in order for the

core loss analysis to be carried out. The dc and ac fluxes in each core leg will be analysed separately.

First, the dc fluxes in the individual core legs are discussed. According to Figure 5.6(a), the instantaneous fluxes in the three core legs in State (1) are restricted by Equations (5.18), (5.51) and (5.52):

$$\Re_o \phi_1 + \Re_o \phi_2 = N_p (i_1 + i_2) = N_p i_{IN} \tag{5.51}$$

$$\Re_o \phi_1 - \Re_c \phi_c = N_s i_s \tag{5.52}$$

Assuming that Φ_1, Φ_2, Φ_c, I_{IN} and $I_{s,1}$ are respectively the dc components of ϕ_1, ϕ_2, ϕ_c, i_{IN} and i_s in State (1), Equations (5.18), (5.51) and (5.52) can be rewritten with the dc components of the variables as:

$$\Re_o \Phi_1 + \Re_o \Phi_2 = N_p I_{IN} \tag{5.53}$$

$$\Re_o \Phi_1 - \Re_c \Phi_c = N_s I_{s,1} \tag{5.54}$$

$$\Phi_c = \Phi_2 - \Phi_1 \tag{5.55}$$

As the converter operation is half cycle symmetrical, the average powers at the transformer secondary and the output must be equal over a half switching period that includes States (1) and (2). The equation of the power balance is:

$$\frac{V_O}{2} \cdot \frac{I_{s,1}(1-D_s)T_s}{T_s/2} = V_O I_O \tag{5.56}$$

Solving for $I_{s,1}$ yields:

$$I_{s,1} = \frac{I_O}{1-D_s} \tag{5.57}$$

The power balance at the input and the output gives:

$$EI_{IN} = V_O I_O \tag{5.58}$$

Manipulations of Equations (5.50), (5.57) and (5.58) yields:

$$I_{s,1} = \frac{N_p}{N_s} \cdot \frac{I_{IN}}{2} \tag{5.59}$$

Substitution of Equation (5.59) to (5.54) yields:

$$\Re_o \Phi_1 - \Re_c \Phi_c = \frac{N_p I_{IN}}{2} \tag{5.60}$$

As Φ_1, Φ_2, Φ_c and I_{IN} are also the dc components of ϕ_1, ϕ_2, ϕ_c and i_{IN} over the entire switching period, Equations (5.53), (5.55) and (5.60) are valid over the entire switching period and the dc fluxes in the individual core legs can be solved as:

$$\Phi_1 = \Phi_2 = \frac{N_p I_{IN}}{2\Re_o} \tag{5.61}$$

$$\Phi_c = 0 \tag{5.62}$$

From Equations (5.23) and (5.32), the ac fluxes in the two outer core legs can be calculated as:

$$\left|\Delta\phi_1\right| = \left|\Delta\phi_2\right| = \frac{ED_sT_s}{N_p} \tag{5.63}$$

where $\Delta\phi_1$ and $\Delta\phi_2$ are respectively the total changes of the fluxes in the two outer core legs.

If $\Delta\phi_{1,1}$, $\Delta\phi_{2,1}$ and $\Delta\phi_{c,1}$ are respectively defined as the changes of the fluxes in the individual core legs in State (1) and $\Delta\phi_{1,2}$, $\Delta\phi_{2,2}$ and $\Delta\phi_{c,2}$ are respectively defined as those in State (2), they can be calculated as:

$$\Delta\phi_{1,1} = -\frac{ED_sT_s}{N_p} \tag{5.64}$$

$$\Delta\phi_{2,1} = \frac{E(1-D_s)T_s}{N_p} \tag{5.65}$$

$$\Delta\phi_{c,1} = \Delta\phi_{2,1} - \Delta\phi_{1,1} = \frac{ET_s}{N_p} \tag{5.66}$$

$$\Delta\phi_{1,2} = \Delta\phi_{2,2} = \frac{E\left(D_s - \frac{1}{2}\right)T_s}{N_p} \tag{5.67}$$

$$\Delta\phi_{c,2} = \Delta\phi_{2,2} - \Delta\phi_{1,2} = 0 \tag{5.68}$$

As the flux in the centre core leg starts to decrease in State (3) and both the fluxes in the two outer core legs change monotonically in either States (1) or (2), the total change of the flux in the centre core leg is:

$$\Delta\phi_c = \Delta\phi_{c,1} + \Delta\phi_{c,2} = \frac{ET_s}{N_p} \tag{5.69}$$

Therefore, the ac flux in the centre core leg is:

$$\left|\Delta\phi_c\right| = \frac{ET_s}{N_p} \tag{5.70}$$

From Equations (5.61) to (5.63) and (5.70), the peak flux density in each core leg can be calculated as:

$$B_{1,\max} = B_{2,\max} = \frac{N_p I_{IN}}{\Re_o A_c} + \frac{ED_s T_s}{N_p A_c} \tag{5.71}$$

$$B_{c,\max} = \frac{ET_s}{2N_p A_c} \tag{5.72}$$

where A_c is the cross section area of the centre core leg. The cross section area of the outer core leg is normally made to be half that of the centre core leg in ETD core types.

The flux waveforms are shown in Figure 5.7. It can be seen that the dc fluxes in the two outer core legs are cancelled while the ac fluxes are added together in the centre core leg.

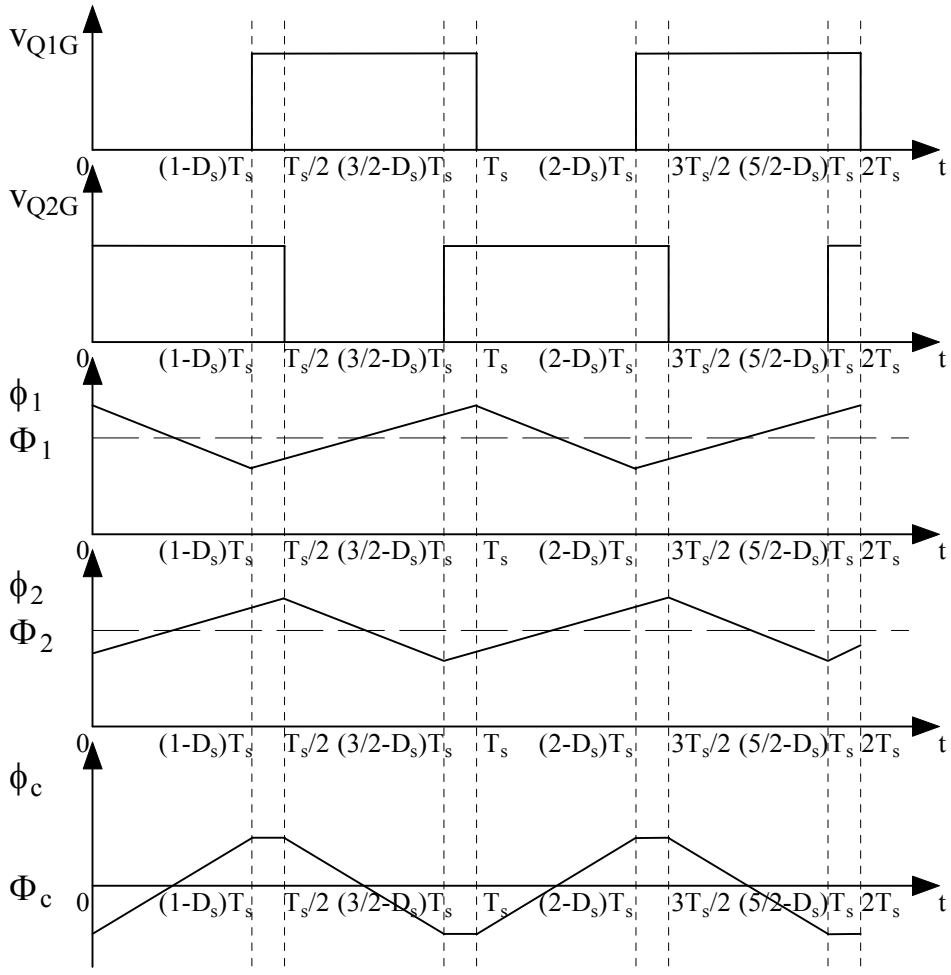

Figure 5.7 Flux Waveforms in Structure A Core

5.2.5 Current Ripples

The current ripples in the MOSFETs and the magnetic windings affect the conduction losses because under the same level of the dc component, the effective current increases if the ripple current is higher.

If $\Delta i_{IN,1}$ and $\Delta i_{s,1}$ are respectively defined as the changes of the input and the transformer secondary currents i_{IN} and i_s in State (1), Equations (5.51) and (5.52) can be rewritten with the ac components of the variables in State (1) as:

$$\Delta i_{IN,1} = \frac{\Re_o \Delta \phi_{1,1} + \Re_o \Delta \phi_{2,1}}{N_p} \tag{5.73}$$

$$\Delta i_{s,1} = \frac{\Re_o \Delta \phi_{1,1} - \Re_c \Delta \phi_{c,1}}{N_s} \tag{5.74}$$

As the input current starts to decrease in State (2) and the transformer secondary current is zero in State (2), $\Delta i_{IN,1}$ and $\Delta i_{s,1}$ are also Δi_{IN} and Δi_s, the total changes of i_{IN} and i_s. Substitution of Equations (5.64), (5.65) and (5.66) to (5.73) and (5.74) yields:

$$\Delta i_{IN} = \Delta i_{IN,1} = \frac{(1-2D_s)\Re_o E T_s}{N_p^2} \tag{5.75}$$

$$\Delta i_s = \Delta i_{s,1} = -\frac{N_p}{N_s} \cdot \frac{(D_s \Re_o + \Re_c) E T_s}{N_p^2} \tag{5.76}$$

If $\Delta i_{1,1}$, $\Delta i_{p,1}$, $\Delta i_{s1,1}$ and $\Delta i_{s2,1}$ are respectively defined as the changes of the currents i_1, i_p, i_{s1} and i_{s2} in State (1), Equations (5.5), (5.6), (5.8) and (5.9) can be rewritten with the ac variables in State (1) as:

$$\Delta i_{s1,1} = \frac{N_p}{N_s} \Delta i_{p,1} \tag{5.77}$$

$$\Delta i_{p,1} = \Delta i_{1,1} \tag{5.78}$$

$$\Delta i_{s2,1} = -\frac{v_{s,1}(1-D_s)T_s}{L_{ms}} \tag{5.79}$$

$$\Delta i_{s,1} = \Delta i_{s1,1} + \Delta i_{s2,1} \tag{5.80}$$

Substitution of Equations (5.44), (5.45), (5.50) and (5.76) to (5.77), (5.78), (5.79) and (5.80) yields:

$$\Delta i_{1,1} = -\frac{D_s \Re_o E T_s}{N_p^2} \tag{5.81}$$

As the current i_1 starts to increase in State (2) and the converter operation is half cycle symmetrical, $\Delta i_{1,1}$ is also Δi_1 or Δi_2, the total change of i_1 or i_2. The current ripples of i_{IN}, i_1, i_2 and i_s are respectively:

$$\left|\Delta i_{IN}\right| = \frac{(2D_s - 1)\Re_o E T_s}{N_p^2} \tag{5.82}$$

$$\left|\Delta i_1\right| = \left|\Delta i_2\right| = \frac{D_s \Re_o E T_s}{N_p^2} \tag{5.83}$$

$$\left|\Delta i_s\right| = \frac{N_p}{N_s} \cdot \frac{(D_s \Re_o + \Re_c) E T_s}{N_p^2} \tag{5.84}$$

The current waveforms are the same as those in the converter with discrete magnetics shown in Figure 5.4.

5.3 Integrated Magnetics with Winding Integration

In order to further reduce the number of interconnections between the individual windings as well as the copper loss and the winding cost, winding integration is proposed as a better approach in magnetic integration [155]. This section studies three magnetic integration solutions with winding integration technique for the two-inductor boost converter.

5.3.1 Winding Integration Technique

In the two-inductor boost converter, the transformer primary winding can be merged with the individual inductor windings and the two combined windings must be located on the two outer legs of a three-leg core to achieve the symmetrical operation. Each combined winding functions as both the input inductor and the transformer primary windings in the converter with discrete magnetics. Topographically, there are four ways to wind the two combined windings onto the

two outer core legs and the directions of the induced fluxes ϕ_1 and ϕ_2 have four different combinations as shown in Figure 5.8.

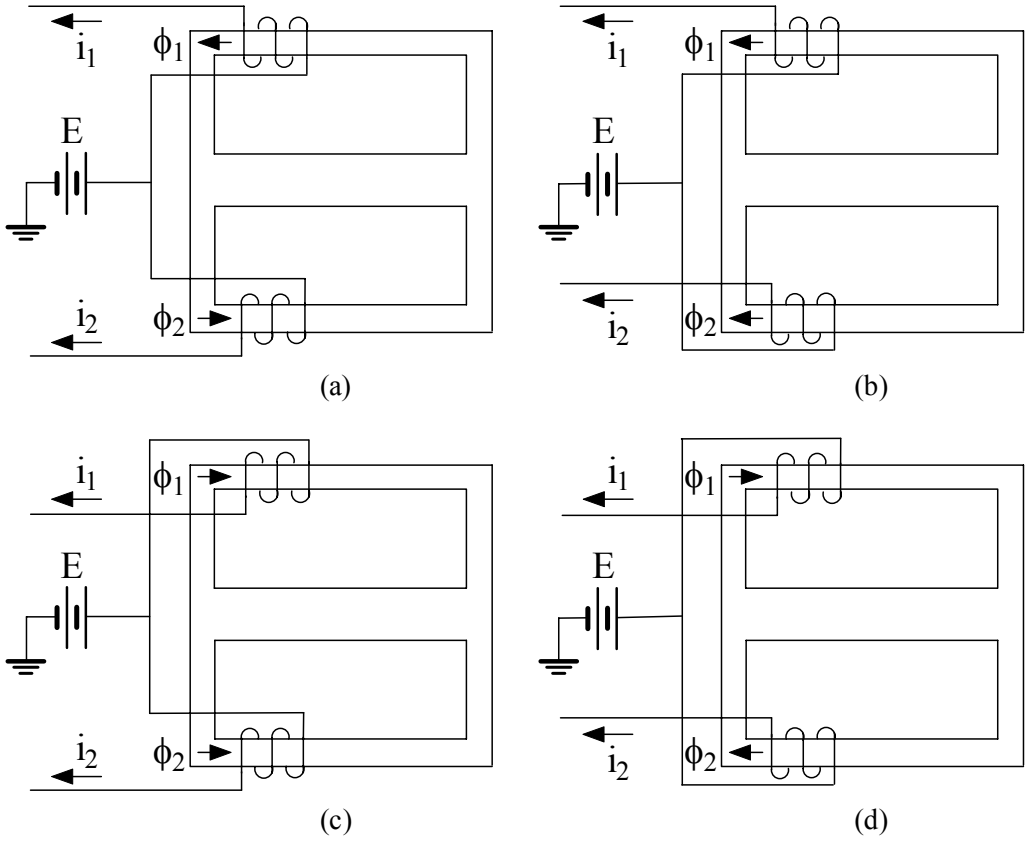

Figure 5.8 Four Ways to Wind the Two Combined Windings

According to the directions of the flux changes in the individual core legs, the number of the winding structures can be finally reduced to two, as shown in Figures 5.8(a) and (b). The winding structure in Figure 5.8(c) is equivalent to that in Figure 5.8(b) while that in Figure 5.8(d) is equivalent to that in Figure 5.8(a). In Figure 5.8(a), the flux changes generated by the two individual windings are of the same direction in the two outer core legs and of different directions in the centre core leg. In Figure 5.8(b), the flux changes generated by the two individual windings are of

different directions in the two outer core legs and of the same direction in the centre core leg.

As the flux in the transformer secondary winding must be alternating, the secondary winding must be placed on the centre core leg in Figure 5.8(a) and on the two outer core legs in Figure 5.8(b). In these arrangements, the currents in the two windings on the outer core legs can be alternatively switched on so that an alternating flux can be generated in the transformer secondary winding.

5.3.2 Structure B Magnetic Integration

The approach which uses single secondary winding on the centre core leg is named as Structure B, as shown in Figure 5.9. In Figure 5.9, the locations of the MOSFETs Q_1 and Q_2 are changed and Q_1 is in series with the bottom combined winding while Q_2 is in series with the top combined winding. This arrangement maintains the relationship of the closings of the MOSFETs and the direction of the transformer secondary current. In the two-inductor boost converter with discrete magnetics, the closing of Q_2 results in a positive transformer secondary current as illustrated in Figure 5.1. In the converter with integrated magnetics, the windings on the outer core legs integrate the functions of the input inductor and the transformer primary windings and the closing of Q_2 also results in a positive transformer secondary current as illustrated in Figure 5.9. The magnetic circuits of Structure B in different states are drawn in Figure 5.10.

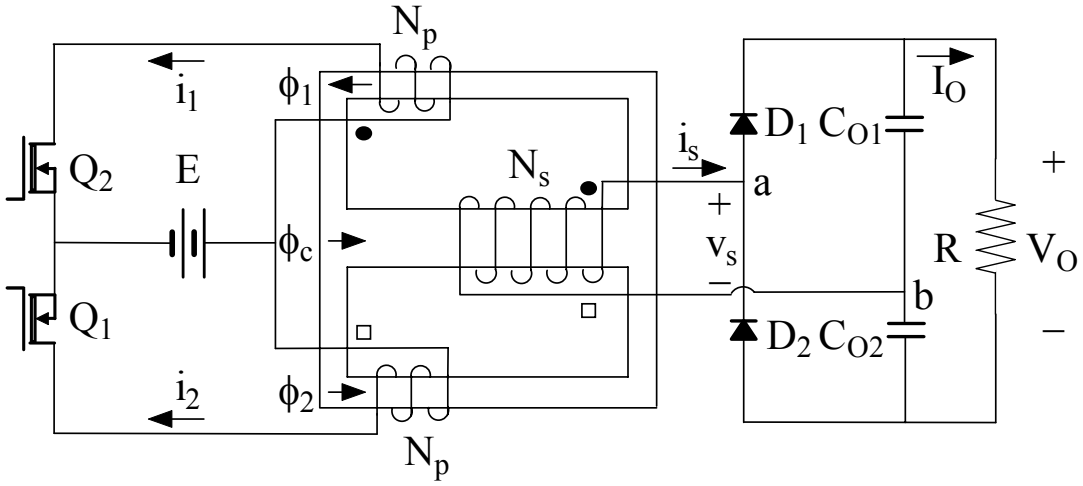

Figure 5.9 Two-Inductor Boost Converter with Structure B Magnetic Integration

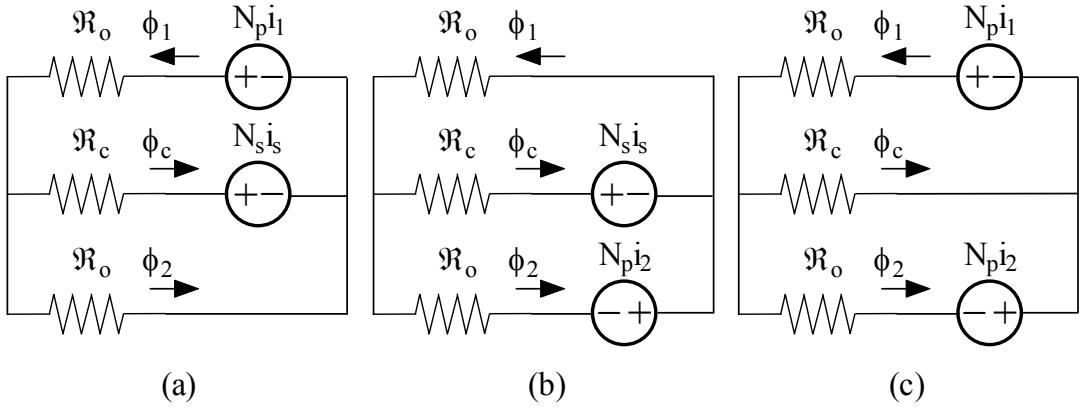

Figure 5.10 Structure B Magnetic Circuits

(a) State (1) (b) State (3) (c) States (2) and (4)

The converter is now analysed under three different operating conditions.

- State (1) ($v_s > 0$)

In this state, Q_1 is off while Q_2 is on and $i_2 = 0$. The fluxes in one outer and the

centre core legs are respectively:

$$\phi_1 = \frac{N_p i_1}{\Re_o + 2\Re_c}\left(1 + \frac{\Re_c}{\Re_o}\right) - \frac{N_s i_s}{\Re_o + 2\Re_c} \tag{5.85}$$

$$\phi_c = \frac{N_p i_1}{\Re_o + 2\Re_c} - \frac{2N_s i_s}{\Re_o + 2\Re_c} \tag{5.86}$$

According to Figure 5.9, Faraday's Law gives Equations (5.32) and (5.40). Substitution of Equations (5.85) and (5.86) to (5.32) and (5.40) yields Equations (5.28) and (5.29).

- State (3) ($v_s < 0$)

In this state, Q_1 is on while Q_2 is off and $i_1 = 0$. The fluxes in one outer and the centre core legs are respectively:

$$\phi_2 = \frac{N_p i_2}{\Re_o + 2\Re_c}\left(1 + \frac{\Re_c}{\Re_o}\right) + \frac{N_s i_s}{\Re_o + 2\Re_c} \tag{5.87}$$

$$\phi_c = -\frac{N_p i_2}{\Re_o + 2\Re_c} - \frac{2N_s i_s}{\Re_o + 2\Re_c} \tag{5.88}$$

According to Figure 5.9, Faraday's Law gives Equations (5.23) and (5.40). Substitution of Equations (5.87) and (5.88) to (5.23) and (5.40) yields Equations (5.36) and (5.37).

- States (2) and (4) ($v_s = 0$)

In these two states, Q_1 and Q_2 are both on. According to Figure 5.9, Faraday's Law gives Equations (5.23), (5.32) and (5.40). The fluxes in the individual core legs also obey the following equation:

$$\phi_1 = \phi_2 + \phi_c \tag{5.89}$$

The fluxes in the two outer core legs are respectively given in Equations (5.38) and (5.39) and substitution of Equations (5.38) and (5.39) to (5.23) and (5.32) yields Equation (5.41). Manipulations of Equations (5.23), (5.32), (5.40) and (5.89) yield Equation (5.12). Therefore, Equation (5.13) is still valid in this state.

As the derivatives of the input and the transformer secondary currents in the individual operating conditions in Structure B are the same as those in Structure A, the equivalent input inductances and magnetising inductance are the same as those given in Equations (5.43) and (5.44). Therefore, this magnetic structure also requires that the outer core legs be gapped to store the energy in the input inductors. Like the gapping arrangement of the centre core leg in Structure A, the gapping of the centre core leg is possible but not indispensable in Structure B.

5.3.3 Structures C and D Magnetic Integration

The approach which uses two secondary windings on the two outer core legs is named as Structure C, as shown in Figure 5.11 [130], [144], [145]. In Figure 5.11, the MOSFETs Q_1 and Q_2 have the same locations as those in Figure 5.9. The magnetic circuits of Structure C in different states are drawn in Figure 5.12.

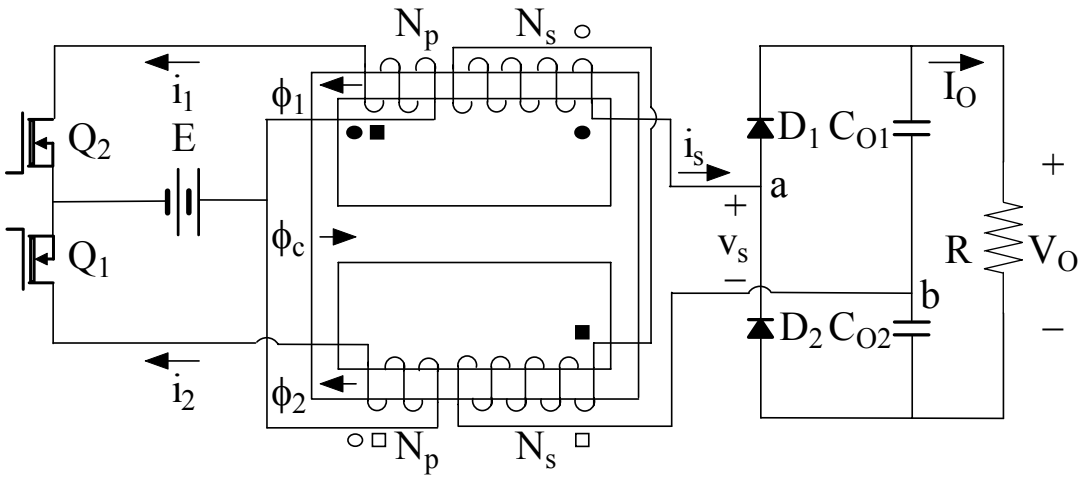

Figure 5.11 Two-Inductor Boost Converter with Structure C Magnetic Integration

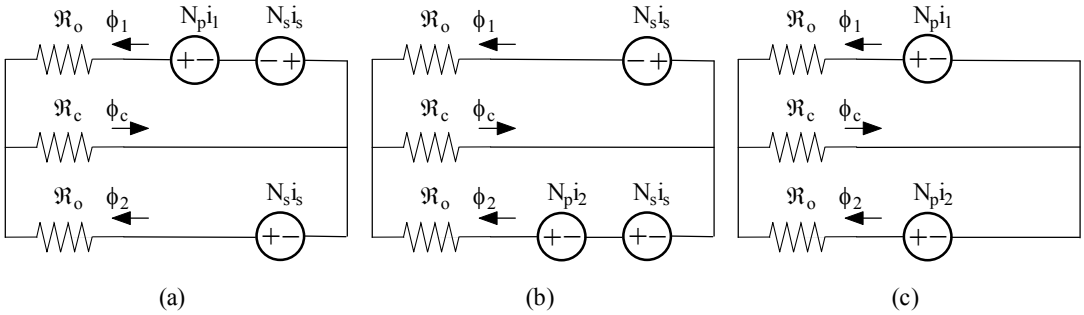

Figure 5.12 Structure C Magnetic Circuits

(a) State (1) (b) State (3) (c) States (2) and (4)

The converter is now analysed under three different operating conditions.

- State (1) ($v_s > 0$)

In this state, Q_1 is off while Q_2 is on and $i_2 = 0$. The fluxes in the two outer core legs are respectively:

$$\phi_1 = \frac{N_p i_1}{\Re_o + 2\Re_c}\left(1 + \frac{\Re_c}{\Re_o}\right) - \frac{N_s i_s}{\Re_o} \tag{5.90}$$

$$\phi_2 = -\frac{N_p i_1}{\Re_o + 2\Re_c} \cdot \frac{\Re_c}{\Re_o} + \frac{N_s i_s}{\Re_o} \tag{5.91}$$

According to Figure 5.11, Faraday's Law gives Equations (5.32) and (5.92):

$$N_s \frac{d\phi_1}{dt} - N_s \frac{d\phi_2}{dt} = v_s \tag{5.92}$$

Substitution of Equations (5.90) and (5.91) to (5.32) and (5.92) yields:

$$\frac{d(i_1 + i_2)}{dt} = \frac{\Re_o + 2\Re_c}{N_p^2}\left(2E - \frac{N_p}{N_s} v_s\right) \tag{5.93}$$

$$\frac{di_s}{dt} = \frac{\Re_o + 2\Re_c}{N_p N_s} E - \frac{\Re_o + \Re_c}{N_s^2} v_s \tag{5.94}$$

By defining L_c and L_d as:

$$L_c = \frac{N_p^2}{\Re_o + 2\Re_c} \tag{5.95}$$

$$L_d = \frac{2N_s^2}{\Re_o} \tag{5.96}$$

Equations (5.93) and (5.94) can be simplified to:

$$\frac{d(i_1 + i_2)}{dt} = \frac{1}{L_c}\left(2E - \frac{N_p}{N_s}v_s\right) \tag{5.97}$$

$$\frac{di_s}{dt} = \frac{N_p}{N_s}\cdot\frac{E}{L_c} - \left[\frac{1}{L_d} + \left(\frac{N_p}{N_s}\right)^2 \frac{1}{2L_c}\right]v_s \tag{5.98}$$

- State (3) ($v_s < 0$)

In this state, Q_1 is on while Q_2 is off and $i_1 = 0$. The fluxes in the two outer core legs are respectively:

$$\phi_1 = -\frac{N_p i_2}{\Re_o + 2\Re_c}\cdot\frac{\Re_c}{\Re_o} - \frac{N_s i_s}{\Re_o} \tag{5.99}$$

$$\phi_2 = \frac{N_p i_2}{\Re_o + 2\Re_c}\left(1 + \frac{\Re_c}{\Re_o}\right) + \frac{N_s i_s}{\Re_o} \tag{5.100}$$

According to Figure 5.11, Faraday's Law gives Equations (5.23) and (5.92). Substitution of Equations (5.99) and (5.100) to (5.23) and (5.92) yields:

$$\frac{d(i_1+i_2)}{dt}=\frac{\Re_o+2\Re_c}{N_p^2}\left(2E+\frac{N_p}{N_s}v_s\right) \tag{5.101}$$

$$\frac{di_s}{dt}=-\frac{\Re_o+2\Re_c}{N_pN_s}E-\frac{\Re_o+\Re_c}{N_s^2}v_s \tag{5.102}$$

Equations (5.101) and (5.102) can be simplified by the definitions of L_c and L_d in Equations (5.95) and (5.96) to:

$$\frac{d(i_1+i_2)}{dt}=\frac{1}{L_c}\left(2E+\frac{N_p}{N_s}v_s\right) \tag{5.103}$$

$$\frac{di_s}{dt}=-\frac{N_p}{N_s}\cdot\frac{E}{L_c}-\left[\frac{1}{L_d}+\left(\frac{N_p}{N_s}\right)^2\frac{1}{2L_c}\right]v_s \tag{5.104}$$

- States (2) and (4) ($v_s=0$)

In these two states, Q_1 and Q_2 are both on. The fluxes in the two outer core legs are respectively:

$$\phi_1=\frac{N_pi_1}{\Re_o+2\Re_c}\left(1+\frac{\Re_c}{\Re_o}\right)-\frac{N_pi_2}{\Re_o+2\Re_c}\cdot\frac{\Re_c}{\Re_o} \tag{5.105}$$

$$\phi_2 = -\frac{N_p i_1}{\Re_o + 2\Re_c} \cdot \frac{\Re_c}{\Re_o} + \frac{N_p i_2}{\Re_o + 2\Re_c}\left(1 + \frac{\Re_c}{\Re_o}\right) \tag{5.106}$$

According to Figure 5.11, Faraday's Law gives Equations (5.23), (5.32) and (5.92). The fluxes in the individual core legs also obey the following equation:

$$\phi_c = \phi_1 + \phi_2 \tag{5.107}$$

Substitution of Equations (5.105) and (5.106) to (5.23) and (5.32) yields:

$$\frac{d(i_1 + i_2)}{dt} = \frac{\Re_o + 2\Re_c}{N_p^2} 2E \tag{5.108}$$

Equation (5.108) can be simplified by the definition of L_c in Equation (5.95) to:

$$\frac{d(i_1 + i_2)}{dt} = \frac{1}{L_c} 2E \tag{5.109}$$

Manipulations of Equations (5.23), (5.32), (5.92) and (5.107) yield Equation (5.12). Therefore, Equation (5.13) is still valid in this state.

Comparisons of Equations (5.97), (5.98), (5.103), (5.104) and (5.109) respectively with their discrete magnetic counterparts, Equations (5.4), (5.10), (5.14), (5.15) and (5.11), yield:

$$L = L_c = \frac{N_p^2}{\Re_o + 2\Re_c} \tag{5.110}$$

$$L_{ms} = \frac{1}{\frac{1}{L_d} - \left(\frac{N_p}{N_s}\right)^2 \frac{1}{2L_c}} = -\frac{N_s^2}{\Re_c} \tag{5.111}$$

Equations (5.110) and (5.111) imply that other than the number of turns, the input inductances are related to the reluctances of both the outer and the centre core legs and the magnetising inductance is inversely proportional to that of the centre core leg only. In this magnetic structure, the centre core leg can be gapped to store the energy in the input inductors. The gapping of the outer core legs is possible but not indispensable. If the centre core leg is the only gapped leg, the input inductances can be estimated to be inversely proportional to the reluctance of the centre core leg as $\Re_c >> \Re_o$ in this case.

According to the flux directions specified in Structure C in Figure 5.11, the increase or the decrease of the flux in the centre core leg results in the increase or the decrease of both the fluxes in the two outer core legs. Therefore, a variation of this magnetic structure can be developed by placing another winding in the centre core leg in series with one of the two combined windings in the converter primary side when only one MOSFET is on. This approach is named as Structure D. Figure 5.13 shows the circuit diagram of the two-inductor boost converter with Structure D magnetic integration. The magnetic circuits of Structure D in different states are drawn in Figure 5.14.

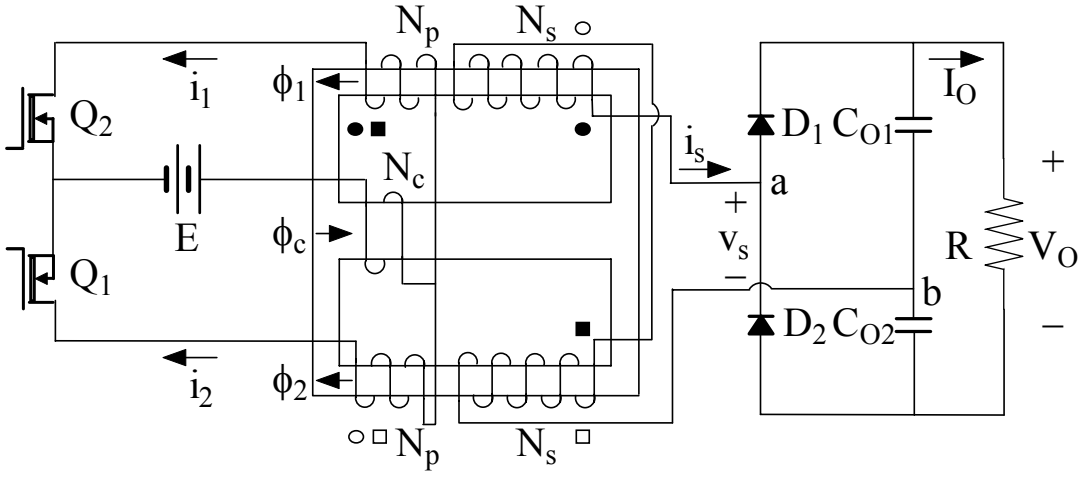

Figure 5.13 Two-Inductor Boost Converter with Structure D Magnetic Integration

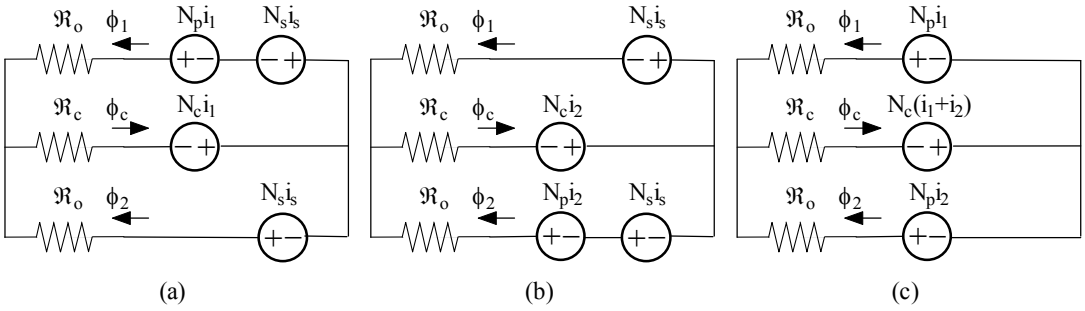

Figure 5.14 Structure D Magnetic Circuits

(a) State (1) (b) State (3) (c) States (2) and (4)

The converter is now analysed under three different operating conditions.

- State (1) ($v_s > 0$)

In this state, Q_1 is off while Q_2 is on and $i_2 = 0$. If N_c is the number of the turns of the centre core leg winding, the fluxes in the three core legs are respectively:

$$\phi_1 = \frac{i_1}{\Re_o + 2\Re_c}\left[N_p\left(1+\frac{\Re_c}{\Re_o}\right) + N_c \right] - \frac{N_s i_s}{\Re_o} \tag{5.112}$$

$$\phi_2 = \frac{i_1}{\Re_o + 2\Re_c}\left(- N_p \frac{\Re_c}{\Re_o} + N_c \right) + \frac{N_s i_s}{\Re_o} \tag{5.113}$$

$$\phi_c = \frac{(N_p + 2N_c) i_1}{\Re_o + 2\Re_c} \tag{5.114}$$

According to Figure 5.13, Faraday's Law gives Equations (5.92) and (5.115):

$$N_p \frac{d\phi_1}{dt} + N_c \frac{d\phi_c}{dt} = E \tag{5.115}$$

Substitution of Equations (5.112), (5.113) and (5.114) to (5.92) and (5.115) yields:

$$\frac{d(i_1 + i_2)}{dt} = \frac{\Re_o + 2\Re_c}{(N_p + 2N_c)^2}\left(2E - \frac{N_p}{N_s} v_s \right) \tag{5.116}$$

$$\frac{di_s}{dt} = \frac{N_p}{N_s} \cdot \frac{\Re_o + 2\Re_c}{(N_p + 2N_c)^2} E - \left[\frac{\Re_o}{2N_s^2} + \left(\frac{N_p}{N_s} \right)^2 \frac{\Re_o + 2\Re_c}{2(N_p + 2N_c)^2} \right] v_s \tag{5.117}$$

With the definition of L_d in Equation (5.96) and by defining L_e as:

$$L_e = \frac{(N_p + 2N_c)^2}{\Re_o + 2\Re_c} \tag{5.118}$$

Equations (5.116) and (5.117) can be simplified to:

$$\frac{d(i_1 + i_2)}{dt} = \frac{1}{L_e}\left(2E - \frac{N_p}{N_s} v_s\right) \tag{5.119}$$

$$\frac{di_s}{dt} = \frac{N_p}{N_s} \cdot \frac{E}{L_e} - \left[\frac{1}{L_d} + \left(\frac{N_p}{N_s}\right)^2 \frac{1}{2L_e}\right] v_s \tag{5.120}$$

- State (3) ($v_s < 0$)

In this state, Q_1 is on while Q_2 is off and $i_1 = 0$. The fluxes in the three core legs are respectively:

$$\phi_1 = \frac{i_2}{\Re_o + 2\Re_c}\left(-N_p \frac{\Re_c}{\Re_o} + N_c\right) - \frac{N_s i_s}{\Re_o} \tag{5.121}$$

$$\phi_2 = \frac{i_2}{\Re_o + 2\Re_c}\left[N_p\left(1 + \frac{\Re_c}{\Re_o}\right) + N_c\right] + \frac{N_s i_s}{\Re_o} \tag{5.122}$$

$$\phi_c = \frac{(N_p + 2N_c) i_2}{\Re_o + 2\Re_c} \tag{5.123}$$

According to Figure 5.13, Faraday's Law gives Equations (5.92) and (5.124):

$$N_p \frac{d\phi_2}{dt} + N_c \frac{d\phi_c}{dt} = E \tag{5.124}$$

Substitution of Equations (5.121), (5.122) and (5.123) to (5.92) and (5.124) yields:

$$\frac{d(i_1+i_2)}{dt}=\frac{\Re_o+2\Re_c}{(N_p+2N_c)^2}\left(2E+\frac{N_p}{N_s}v_s\right) \tag{5.125}$$

$$\frac{di_s}{dt}=-\frac{N_p}{N_s}\cdot\frac{\Re_o+2\Re_c}{(N_p+2N_c)^2}E-\left[\frac{\Re_o}{2N_s^2}+\left(\frac{N_p}{N_s}\right)^2\frac{\Re_o+2\Re_c}{2(N_p+2N_c)^2}\right]v_s \tag{5.126}$$

Equations (5.125) and (5.126) can be simplified with the definitions of L_d and L_e in Equations (5.96) and (5.118) to:

$$\frac{d(i_1+i_2)}{dt}=\frac{1}{L_e}\left(2E+\frac{N_p}{N_s}v_s\right) \tag{5.127}$$

$$\frac{di_s}{dt}=-\frac{N_p}{N_s}\cdot\frac{E}{L_e}-\left[\frac{1}{L_d}+\left(\frac{N_p}{N_s}\right)^2\frac{1}{2L_e}\right]v_s \tag{5.128}$$

- States (2) and (4) ($v_s=0$)

In these two states, Q_1 and Q_2 are both on. The fluxes in the three core legs are respectively:

$$\phi_1=\frac{i_1}{\Re_o+2\Re_c}\left[N_p\left(1+\frac{\Re_c}{\Re_o}\right)+N_c\right]-\frac{i_2}{\Re_o+2\Re_c}\left(N_p\frac{\Re_c}{\Re_o}-N_c\right) \tag{5.129}$$

$$\phi_2 = \frac{i_1}{\Re_o + 2\Re_c}\left(-N_p\frac{\Re_c}{\Re_o} + N_c\right) + \frac{i_2}{\Re_o + 2\Re_c}\left[N_p\left(1+\frac{\Re_c}{\Re_o}\right) + N_c\right] \quad (5.130)$$

$$\phi_c = \frac{(N_p + 2N_c)(i_1 + i_2)}{\Re_o + 2\Re_c} \quad (5.131)$$

According to Figure 5.13, Equations (5.92), (5.107), (5.115) and (5.124) can be established. Substitution of Equations (5.129), (5.130) and (5.131) to (5.115) and (5.124) yields:

$$\frac{d(i_1 + i_2)}{dt} = \frac{\Re_o + 2\Re_c}{(N_p + 2N_c)^2}2E \quad (5.132)$$

Equation (5.132) can be simplified by the definition of L_e in Equation (5.118) as:

$$\frac{d(i_1 + i_2)}{dt} = \frac{1}{L_e}2E \quad (5.133)$$

Manipulations of Equations (5.92), (5.107), (5.115) and (5.124) yield Equation (5.12). Therefore, Equation (5.13) is still valid in this state.

Comparisons of Equations (5.119), (5.120), (5.127), (5.128) and (5.133) respectively with their discrete magnetic counterparts, Equations (5.4), (5.10), (5.14), (5.15) and (5.11), yield:

$$L = L_e = \frac{(N_p + 2N_c)^2}{\Re_o + 2\Re_c} \tag{5.134}$$

$$L_{ms} = \frac{1}{\frac{1}{L_d} - \left(\frac{N_p}{N_s}\right)^2 \frac{1}{2L_e}} = \frac{2N_s^2}{\Re_o - \left(\frac{N_p}{N_p + 2N_c}\right)^2 (\Re_o + 2\Re_c)} \tag{5.135}$$

Equations (5.134) and (5.135) imply that other than the number of turns, the input and the magnetising inductances are related to the reluctances of both the outer and the centre core legs. In this magnetic structure, the gapping arrangement is the same as that in Structure C and the input inductances can be estimated to be inversely proportional to the reluctance of the centre core leg if only the centre core leg is gapped. The extra winding on the centre core leg in this magnetic integration structure provides additional input filtering inductance to the input current and one winding turn on the centre core leg is effective as two winding turns on the outer core leg in the contribution to the input inductances according to Equation (5.134).

5.4 Comparisons of the Four Magnetic Integration Structures

In this section, a set of parameters including the dc gain, the dc and ac flux densities in the three core legs and the current ripples in the individual windings will be established and comparisons will be made for the four magnetic structures.

5.4.1 Structure A Magnetic Integration

The individual parameters have been established in Section 5.2 and will not be repeated here. The parameters of the remaining three magnetic structures will be derived with the same approaches.

5.4.2 Structure B Magnetic Integration

According to Figure 5.9, Faraday's Law gives Equations (5.23) and (5.40) in State (3) when Q_2 is off and Equation (5.32) in States (1), (2) and (4) when Q_2 is on. Manipulations of Equations (5.23), (5.40) and (5.89) yield:

$$N_p \frac{d\phi_1}{dt} = E + \frac{N_p}{N_s} v_s \tag{5.136}$$

In State (3), the transformer secondary voltage can be found as:

$$v_s = v_{s,3} = -\frac{V_O}{2} \tag{5.137}$$

Therefore, Equation (5.136) can be rewritten as Equation (5.46). The change of the flux when Q_2 is off, $(\Delta\phi_1)_{Q2,off}$ and that when Q_2 is on, $(\Delta\phi_1)_{Q2,on}$, are respectively:

$$(\Delta\phi_1)_{Q2,off} = \frac{\left(E - \frac{N_p}{N_s} \cdot \frac{V_O}{2}\right)(1-D_s)T_s}{N_p} \tag{5.138}$$

$$(\Delta\phi_1)_{Q2,on} = \frac{ED_sT_s}{N_p} \tag{5.139}$$

Due to the continuity of the flux, the following equation can be obtained:

$$(\Delta\phi_1)_{Q2,off} + (\Delta\phi_1)_{Q2,on} = 0 \tag{5.140}$$

Substitution of Equations (5.138) and (5.139) to (5.140) and solving for V_O yield Equation (5.50).

According to Figure 5.10(a), the instantaneous fluxes in the three core legs in State (1) are restricted by Equations (5.89), (5.141) and (5.142):

$$\Re_o\phi_1 + \Re_o\phi_2 = N_p i_1 = N_p i_{IN} \tag{5.141}$$

$$\Re_o\phi_2 - \Re_c\phi_c = N_s i_s \tag{5.142}$$

Equations (5.141), (5.142) and (5.89) can be respectively rewritten with the dc components of the variables as Equations (5.53), (5.143) and (5.144), which are valid over the entire switching period:

$$\Re_o \Phi_2 - \Re_c \Phi_c = \frac{N_p I_{IN}}{2} \tag{5.143}$$

$$\Phi_1 = \Phi_2 + \Phi_c \tag{5.144}$$

The dc fluxes in the individual core legs can be calculated from Equations (5.53), (5.143) and (5.144) and they are the same as those in Structure A, which are given in Equations (5.61) and (5.62).

The ac fluxes in the two outer core legs are the same as those in Structure A, which are given in (5.63). The changes of the fluxes in the individual core legs in State (1) $\Delta\phi_{1,1}$, $\Delta\phi_{2,1}$ and $\Delta\phi_{c,1}$ are respectively:

$$\Delta\phi_{1,1} = \frac{E(1-D_s)T_s}{N_p} \tag{5.145}$$

$$\Delta\phi_{2,1} = -\frac{ED_sT_s}{N_p} \tag{5.146}$$

$$\Delta\phi_{c,1} = \Delta\phi_{1,1} - \Delta\phi_{2,1} = \frac{ET_s}{N_p} \tag{5.147}$$

The changes of the fluxes in the two outer core legs in State (2) $\Delta\phi_{1,2}$ and $\Delta\phi_{2,2}$ are the same as those in Structure A, which are given in Equation (5.67). The change of the flux in the centre core legs in State (2) $\Delta\phi_{c,2}$ can then be calculated as:

$$\Delta\phi_{c,2} = \Delta\phi_{1,2} - \Delta\phi_{2,2} = 0 \tag{5.148}$$

As the flux in the centre core leg starts to decrease in State (3), the ac flux can be calculated from Equations (5.147) and (5.148). It can be calculated that the ac flux in the centre core leg is the same as that in Structure A, which is given in Equation (5.70). As both the dc and ac fluxes are the same as those in Structure A, the peak flux densities in the individual core legs are the same as those in Structure A, which are given in Equations (5.71) and (5.72).

In order to find the input and the transformer secondary current ripples, Equations (5.141) and (5.142) must be rewritten with the ac components of the variables in State (1) to Equations (5.73) and (5.149):

$$\Delta i_{s,1} = \frac{\Re_o \Delta\phi_{2,1} - \Re_c \Delta\phi_{c,1}}{N_s} \tag{5.149}$$

After substitution of Equations (5.145), (5.146) and (5.147) to (5.73) and (5.149), the current ripples can be found to be the same as those in Structure A, which are given in Equations (5.82) and (5.84).

The flux and the current waveforms are shown in Figure 5.15. It can be seen that in Structure B, the dc fluxes in the two outer core legs are cancelled and the ac fluxes are added together in the centre core leg.

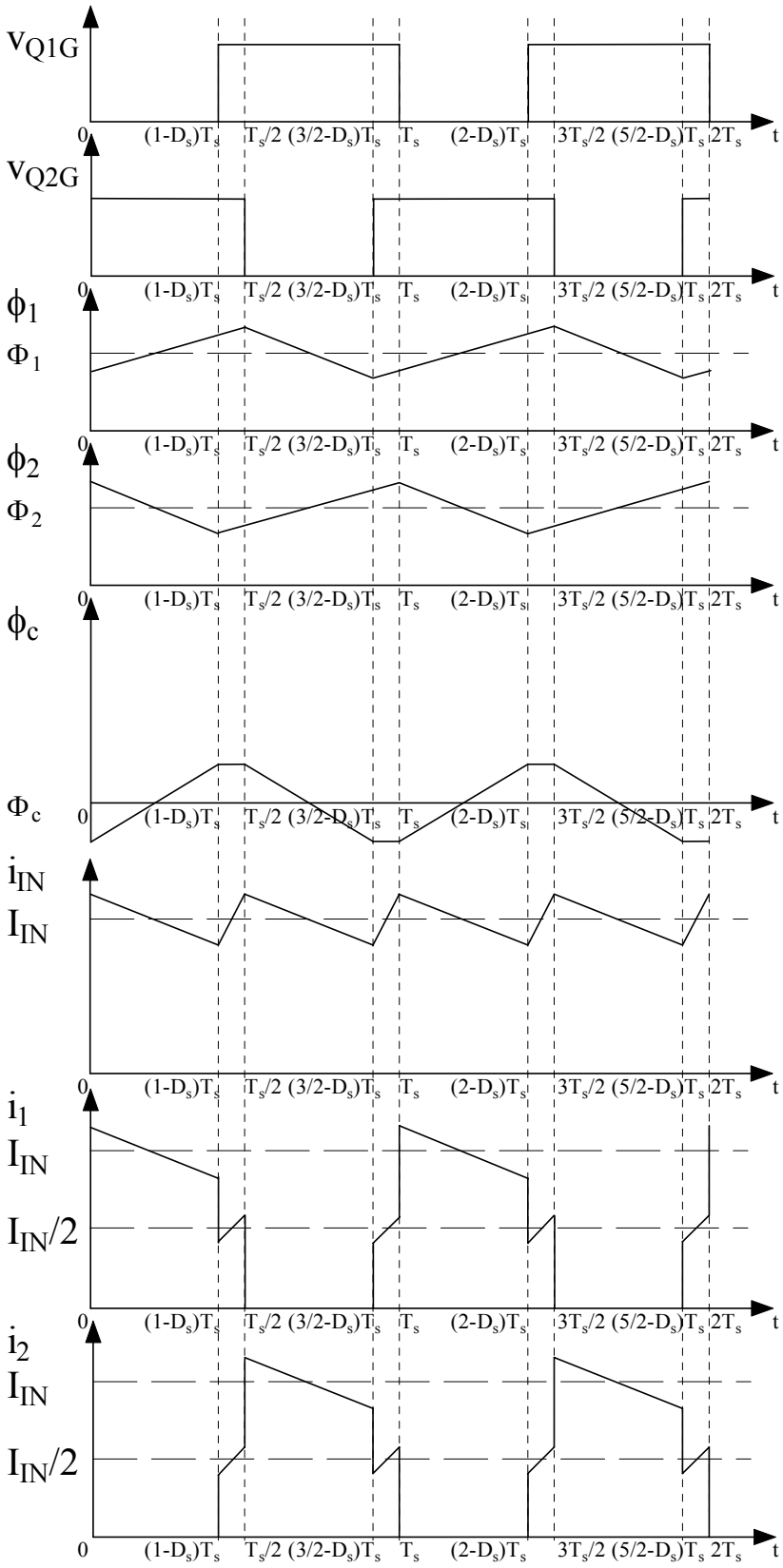

Figure 5.15 Flux and the Current Waveforms in Structure B

5.4.3 Structure C Magnetic Integration

According to Figure 5.11, Faraday's Law gives Equations (5.23) and (5.92) in State (3) when Q_2 is off and Equation (5.32) in States (1), (2) and (4) when Q_2 is on. Manipulations of Equations (5.23) and (5.92) yield Equation (5.136). The change of the flux when Q_2 is off, $(\Delta\phi_1)_{Q2,off}$ and that when Q_2 is on, $(\Delta\phi_1)_{Q2,on}$, are respectively given in Equations (5.138) and (5.139) and the output voltage V_O can be calculated as given in Equation (5.50).

According to Figure 5.12(a), the instantaneous fluxes in the three core legs in State (a) are restricted by Equations (5.107), (5.150) and (5.151):

$$\Re_o\phi_1 + \Re_c\phi_c = N_p i_1 - N_s i_s = N_p i_{IN} - N_s i_s \tag{5.150}$$

$$\Re_o\phi_2 + \Re_c\phi_c = N_s i_s \tag{5.151}$$

Equations (5.107), (5.150) and (5.151) can be respectively rewritten with the dc components of the variables as Equations (5.152) to (5.154), which are valid over the entire switching period:

$$\Re_o\Phi_1 + \Re_c\Phi_c = \frac{N_p I_{IN}}{2} \tag{5.152}$$

$$\Re_o\Phi_2 + \Re_c\Phi_c = \frac{N_p I_{IN}}{2} \tag{5.153}$$

$$\Phi_c = \Phi_1 + \Phi_2 \tag{5.154}$$

The dc fluxes in the individual core legs can be solved as:

$$\Phi_1 = \Phi_2 = \frac{N_p I_{IN}}{2(\Re_o + 2\Re_c)} \tag{5.155}$$

$$\Phi_c = \frac{N_p I_{IN}}{\Re_o + 2\Re_c} \tag{5.156}$$

The ac fluxes in the two outer core legs are the same as those in Structure A, which are given in (5.63). The changes of the fluxes in the individual core legs in State (1) $\Delta\phi_{1,1}$, $\Delta\phi_{2,1}$ are the same as those in Structure B, which are given in Equations (5.145) and (5.146). The change of the flux in the centre core leg in State (1) $\Delta\phi_{c,1}$ can then be calculated as:

$$\Delta\phi_{c,1} = \Delta\phi_{1,1} + \Delta\phi_{2,1} = \frac{E(1-2D_s)T_s}{N_p} \tag{5.157}$$

As the flux in the centre core leg starts to increase in State (2), the total change of the flux in the centre core leg is:

$$\left|\Delta\phi_c\right| = \left|\Delta\phi_{c,1}\right| = \frac{E(2D_s - 1)T_s}{N_p} \tag{5.158}$$

The peak flux densities in the individual core legs can be calculated as:

$$B_{1,\max} = B_{2,\max} = \frac{N_p I_{IN}}{(\Re_o + 2\Re_c)A_c} + \frac{ED_s T_s}{N_p A_c} \tag{5.159}$$

$$B_{c,\max} = \frac{N_p I_{IN}}{(\Re_o + 2\Re_c)A_c} + \frac{E(2D_s - 1)T_s}{2N_p A_c} \tag{5.160}$$

In order to find the input and the transformer secondary current ripples, Equations (5.150) and (5.151) are manipulated and rewritten with the ac components of the variables in State (1) as:

$$\Delta i_{IN,1} = \frac{\Re_o \Delta\phi_{1,1} + \Re_o \Delta\phi_{2,1} + 2\Re_c \Delta\phi_{c,1}}{N_p} \tag{5.161}$$

$$\Delta i_{s,1} = \frac{\Re_o \Delta\phi_{2,1} + \Re_c \Delta\phi_{c,1}}{N_s} \tag{5.162}$$

As $\Delta i_{IN,1}$ and $\Delta i_{s,1}$ are also the total change of the currents i_{IN} and i_s over the entire switching period, substitution of Equations (5.145), (5.146) and (5.157) to (5.161) and (5.162) yields:

$$\Delta i_{IN} = \frac{(1 - 2D_s)(\Re_o + 2\Re_c)ET_s}{N_p^2} \tag{5.163}$$

$$\Delta i_s = -\frac{N_p}{N_s} \cdot \frac{\left[D_s \Re_o + (2D_s - 1)\Re_c\right]ET_s}{N_p^2} \tag{5.164}$$

The input and transformer secondary current ripples are respectively:

$$\left|\Delta i_{IN}\right| = \frac{(2D_s - 1)(\Re_o + 2\Re_c)ET_s}{N_p^2} \tag{5.165}$$

$$\left|\Delta i_s\right| = \frac{N_p}{N_s} \cdot \frac{\left[D_s\Re_o + (2D_s - 1)\Re_c\right]ET_s}{N_p^2} \tag{5.166}$$

The flux and the current waveforms are shown in Figure 5.16. It can be seen that in Structure C, the dc fluxes in the two outer core legs are added together and the ac fluxes are partially cancelled in the centre core leg. This leads to a much lower core loss in the centre core leg as the core loss increases at a rate much faster than the linear relationship of the ac flux density [165]. Structure C therefore becomes a more attractive design than Structures A and B in terms of the core loss. The core saturation will not be an issue since the cross section area of the centre core leg is twice that of the outer core leg. Under the symmetrical operation, the dc flux density in the centre core leg equals to those in the two outer core legs.

5.4.4 Structure D Magnetic Integration

According to Figure 5.13, Equations (5.92), (5.107) and (5.115) are valid in State (1) when Q_2 is on and Q_1 is off. Manipulations of Equations (5.92), (5.107) and (5.115) yield:

$$(N_p + 2N_c)\frac{d\phi_1}{dt} = E + \frac{N_c}{N_s}v_s \tag{5.167}$$

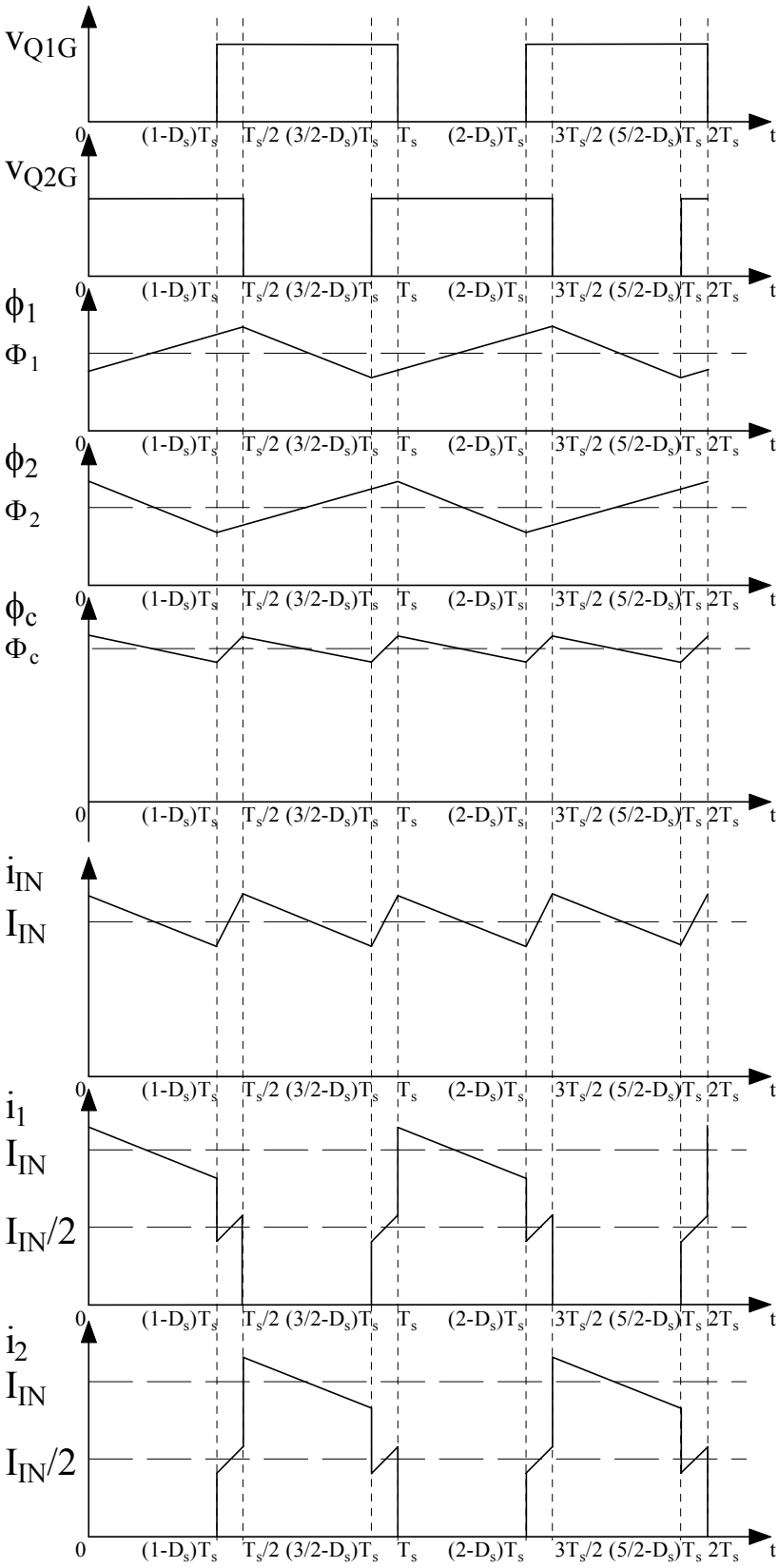

Figure 5.16 Flux and the Current Waveforms in Structure C

Equations (5.107), (5.115) and (5.124) are valid in States (2) and (4) when both Q_1 and Q_2 are on. Manipulations of Equations (5.107), (5.115) and (5.124) yield:

$$(N_p + 2N_c)\frac{d\phi_1}{dt} = E \tag{5.168}$$

Equations (5.92), (5.107) and (5.124) are valid in State (3) when Q_2 is off and Q_1 is on. Manipulations of Equations (5.92), (5.107) and (5.124) yield:

$$(N_p + 2N_c)\frac{d\phi_1}{dt} = E + \frac{N_p + N_c}{N_s}v_s \tag{5.169}$$

As Equations (5.45) and (5.138) are respectively valid in States (1) and (3), the derivatives of the fluxes in Equations (5.167) to (5.169) are constants. If $\Delta\phi_{1,j}$ is defined as the change of the flux in one outer core leg in State (j), where $j = 1,2,3,4$, it can be calculated that:

$$\Delta\phi_{1,1} = \frac{\left(E + \frac{N_c}{N_s}\cdot\frac{V_O}{2}\right)(1-D_s)T_s}{(N_p + 2N_c)} \tag{5.170}$$

$$\Delta\phi_{1,2} + \Delta\phi_{1,4} = \frac{E(2D_s - 1)T_s}{(N_p + 2N_c)} \tag{5.171}$$

$$\Delta\phi_{1,3} = \frac{\left(E - \frac{N_p + N_c}{N_s}\cdot\frac{V_O}{2}\right)(1-D_s)T_s}{(N_p + 2N_c)} \tag{5.172}$$

Due to the continuity of the flux, the following equation can be obtained:

$$\sum_{j=1}^{4} \Delta\phi_{1,j} = 0 \tag{5.173}$$

Substitution of Equations (5.170), (5.171) and (5.172) to (5.173) and solving for V_O yield Equation (5.50). The number of turns of the extra winding in the centre core leg N_c does not appear in the output voltage equation. This implies that while the winding in the centre core leg in Structure D provides additional input inductance, it does not affect the dc gain of the converter. Therefore, this magnetic integration structure offers another degree of freedom in controlling the input current ripples.

According to Figure 5.14(a), the instantaneous fluxes in the three core legs in State (1) are restricted by Equations (5.107), (5.174) and (5.175):

$$\Re_o\phi_1 + \Re_c\phi_c = (N_p + N_c)i_1 - N_s i_s = (N_p + N_c)i_{IN} - N_s i_s \tag{5.174}$$

$$\Re_o\phi_2 + \Re_c\phi_c = N_c i_1 + N_s i_s = N_c i_{IN} + N_s i_s \tag{5.175}$$

Equations (5.107), (5.174) and (5.175) can be respectively rewritten with the dc components of the variables as Equations (5.154), (5.176) and (5.177), which are valid over the entire switching period:

$$\Re_o\Phi_1 + \Re_c\Phi_c = \frac{N_p I_{IN}}{2} + N_c I_{IN} \tag{5.176}$$

$$\Re_o \Phi_2 + \Re_c \Phi_c = \frac{N_p I_{IN}}{2} + N_c I_{IN} \tag{5.177}$$

From Equations (5.154), (5.176) and (5.177), the dc fluxes in the individual core legs can be solved as:

$$\Phi_1 = \Phi_2 = \frac{(N_p + 2N_c) I_{IN}}{2(\Re_o + 2\Re_c)} \tag{5.178}$$

$$\Phi_c = \frac{(N_p + 2N_c) I_{IN}}{\Re_o + 2\Re_c} \tag{5.179}$$

As ϕ_1 increases in States (1), (2) and (4) and decreases in State (3), $\Delta\phi_{1,3}$ is also the total change of the flux in each of the two outer core legs. Substitution of Equation (5.50) to (5.172) yields:

$$\left|\Delta\phi_1\right| = \left|\Delta\phi_2\right| = \left|\Delta\phi_{1,3}\right| = \frac{E\left(D_s + \frac{N_c}{N_p}\right)T_s}{(N_p + 2N_c)} \tag{5.180}$$

The change of the flux in State (1) $\Delta\phi_{2,1}$ is:

$$\Delta\phi_{2,1} = \frac{\left[E - \frac{N_p + N_c}{N_s} \cdot \frac{V_O}{2}\right](1 - D_s)T_s}{(N_p + 2N_c)} \tag{5.181}$$

After substitution of Equation (5.50) to (5.170) and (5.181), the change of the flux in the centre core leg in State (1) $\Delta\phi_{c,1}$ can be calculated as:

$$\Delta\phi_{c,1} = \Delta\phi_{1,1} + \Delta\phi_{2,1} = \frac{E(1-2D_s)T_s}{N_p + 2N_c} \tag{5.182}$$

As the flux in the centre core leg starts to increase in State (2), the total change of the flux in the centre core leg is:

$$\left|\Delta\phi_c\right| = \left|\Delta\phi_{c,1}\right| = \frac{E(2D_s - 1)T_s}{N_p + 2N_c} \tag{5.183}$$

The peak flux densities in the individual core legs can be calculated as:

$$B_{1,\max} = B_{2,\max} = \frac{(N_p + 2N_c)I_{IN}}{(\Re_o + 2\Re_c)A_c} + \frac{E\left(D_s + \frac{N_c}{N_p}\right)T_s}{(N_p + 2N_c)A_c} \tag{5.184}$$

$$B_{c,\max} = \frac{(N_p + 2N_c)I_{IN}}{(\Re_o + 2\Re_c)A_c} + \frac{E(2D_s - 1)T_s}{2(N_p + 2N_c)A_c} \tag{5.185}$$

In order to find the input and the transformer secondary current ripples, Equations (5.174) and (5.175) are rewritten with the ac components of the variables in State (1) as:

$$\Re_o \Delta\phi_{1,1} + \Re_c \Delta\phi_{c,1} = (N_p + N_c)\Delta i_{IN,1} - N_s \Delta i_{s,1} \tag{5.186}$$

$$\Re_o \Delta\phi_{2,1} + \Re \Delta\phi_{c,1} = N_c \Delta i_{IN,1} + N_s \Delta i_{s,1} \tag{5.187}$$

As $\Delta i_{IN,1}$ and $\Delta i_{s,1}$ are also the total changes of the currents i_{IN} and i_s over the entire switching period, manipulations of Equations (5.170), (5.181), (5.182), (5.186) and (5.187) yield:

$$\Delta i_{IN} = \Delta i_{IN,1} = \frac{(1-2D_s)(\Re_o + 2\Re_c)ET_s}{(N_p + 2N_c)^2} \tag{5.188}$$

$$\Delta i_s = \Delta i_{s,1} = -\frac{N_p}{N_s} \cdot \frac{\left[\left(D_s + \frac{2N_c}{N_p} + \frac{2N_c^2}{N_p^2}\right)\Re_o + (2D_s - 1)\Re_c\right]ET_s}{(N_p + 2N_c)^2} \tag{5.189}$$

The input and transformer secondary current ripples are respectively:

$$\left|\Delta i_{IN}\right| = \frac{(2D_s - 1)(\Re_o + 2\Re_c)ET_s}{(N_p + 2N_c)^2} \tag{5.190}$$

$$\left|\Delta i_s\right| = \frac{N_p}{N_s} \cdot \frac{\left[\left(D_s + \frac{2N_c}{N_p} + \frac{2N_c^2}{N_p^2}\right)\Re_o + (2D_s - 1)\Re_c\right]ET_s}{(N_p + 2N_c)^2} \tag{5.191}$$

The flux and the current waveforms are the same as shown in Figure 5.16.

5.4.5 Comparisons

Some important parameters of the four integrated magnetic structures are compared in Table 5.1, where f_s, N_I, N_{II}, N_{III}, $\Re_I$, $\Re_{II}$, $\Re_{III}$, D_I, D_{II}, D_{III}, D_{IV} and D_V are respectively defined as:

$$f_s = \frac{1}{T_s} \tag{5.192}$$

$$N_I = N_p \tag{5.193}$$

$$N_{II} = N_s \tag{5.194}$$

$$N_{III} = N_p + 2N_c \tag{5.195}$$

$$\Re_I = \Re_o \tag{5.196}$$

$$\Re_{II} = \Re_c \tag{5.197}$$

$$\Re_{III} = \Re_o + 2\Re_c \tag{5.198}$$

$$D_I = D_s \tag{5.199}$$

$$D_{II} = 1 - D_s \tag{5.200}$$

$$D_{III} = 2D_s - 1 \tag{5.201}$$

$$D_{IV} = D_s + \frac{N_c}{N_p} \tag{5.202}$$

$$D_V = D_s + \frac{2N_c}{N_p} + \frac{2N_c^2}{N_p^2} \tag{5.203}$$

Item	Structure A	Structure B	Structure C	Structure D
Number of Windings	4	3	4	5
Input Inductance L	$\frac{N_I^2}{\Re_I}$	$\frac{N_I^2}{\Re_I}$	$\frac{N_I^2}{\Re_{III}}$	$\frac{N_{III}^2}{\Re_{III}}$
Magnet-ising Inductance L_{ms}	$\frac{N_{II}^2}{\Re_{II}}$	$\frac{N_{II}^2}{\Re_{II}}$	$-\frac{N_{II}^2}{\Re_{II}}$	$\frac{2N_{II}^2}{\Re_I - \frac{N_I^2}{N_{III}^2}\Re_{III}}$
DC Gain V_O/E	$\frac{N_{II}}{N_I}\cdot\frac{2}{D_{II}}$	$\frac{N_{II}}{N_I}\cdot\frac{2}{D_{II}}$	$\frac{N_{II}}{N_I}\cdot\frac{2}{D_{II}}$	$\frac{N_{II}}{N_I}\cdot\frac{2}{D_{II}}$
Peak Flux Density $B_{1,max}$, $B_{2,max}$	$\frac{N_I I_{IN}}{\Re_I A_c}+\frac{D_I E}{N_I A_c f_s}$	$\frac{N_I I_{IN}}{\Re_I A_c}+\frac{D_I E}{N_I A_c f_s}$	$\frac{N_I I_{IN}}{\Re_{III} A_c}+\frac{D_I E}{N_I A_c f_s}$	$\frac{N_{III} I_{IN}}{\Re_{III} A_c}+\frac{D_{IV} E}{N_{III} A_c f_s}$
Peak Flux Density $B_{c,max}$	$\frac{E}{2N_I A_c f_s}$	$\frac{E}{2N_I A_c f_s}$	$\frac{N_I I_{IN}}{\Re_{III} A_c}+\frac{D_{III} E}{2N_I A_c f_s}$	$\frac{N_{III} I_{IN}}{\Re_{III} A_c}+\frac{D_{III} E}{2N_{III} A_c f_s}$
Current Ripple Δi_{IN}	$\frac{D_{III}\Re_I E}{N_I^2 f_s}$	$\frac{D_{III}\Re_I E}{N_I^2 f_s}$	$\frac{D_{III}\Re_{III} E}{N_I^2 f_s}$	$\frac{D_{III}\Re_{III} E}{N_{III}^2 f_s}$
Current Ripple Δi_s	$\frac{N_I}{N_{II}}\frac{D_I\Re_I+\Re_{II}}{N_I^2 f_s}E$	$\frac{N_I}{N_{II}}\frac{D_I\Re_I+\Re_{II}}{N_I^2 f_s}E$	$\frac{N_I}{N_{II}}\frac{D_I\Re_I+D_{III}\Re_{II}}{N_I^2 f_s}E$	$\frac{N_I}{N_{II}}\frac{D_V\Re_I+D_{III}\Re_{II}}{N_{III}^2 f_s}E$
Leakage Inductance	Low	High	Medium	Medium
Core Loss	High	High	Low	Low
Minimum Gapped Legs	Two outer core legs	Two outer core legs	Centre core leg	Centre core leg

Table 5.1 Comparisons of the Four Integrated Magnetic Structures

5.5 Experimental Waveforms of the Hard-Switched Two-Converter Boost Converter with Structures A and C Magnetic Integration

In order to validate the theoretical analysis, the hard-switched two-inductor boost converter with Structures A and C magnetic integration have been constructed. Structure A is implemented using an ETD39 core with a 0.5-mm air gap in each of the two outer core legs and Structure C is implemented using an ETD39 core with a 0.5-mm air gap in the centre core leg only. The ETD39 core has a minimum centre core leg cross section area of 123 mm^2 [166]. Other main components used in the converter shown in Figures 5.5 and 5.11 are listed below:

- MOSFETs Q_1 and Q_2 – ST STB50NE10, $V_{DS} = 100\ V$, $I_D = 50\ A$, $R_{DS(on)} = 0.027\ \Omega$.
- Diodes D_1 and D_2 – Microsemi UPSC600, $I_F = 1.0\ A$, $V_{RRM} = 600\ V$, $V_F = 1.6\ V$.
- Capacitors C_{O1} and C_{O2} – Vishay class X7R multilayer ceramic surface mount capacitor VJ1210Y104KXCAT, $C = 0.1\ \mu F$, $V_{dc} = 200\ V$.

The ac flux and the current waveforms are respectively shown in Figures 5.17 and 5.18. The top two waveforms are the ac components of the fluxes ϕ_1 and ϕ_c as recovered by integrating the voltage of a single search turn wound on the transformer core leg. The bottom two waveforms are the currents i_1 and i_{IN}.

The experimental waveforms shown in Figure 5.17 agree well with the theoretical waveforms in Figures 5.4 and 5.7 and those shown in Figure 5.18 agree well with the theoretical waveforms in Figure 5.16. It can be clearly seen that for the same amount of flux ripple in the outer core leg, the flux ripple in the centre core leg in Structure C is much smaller than that in Structure A.

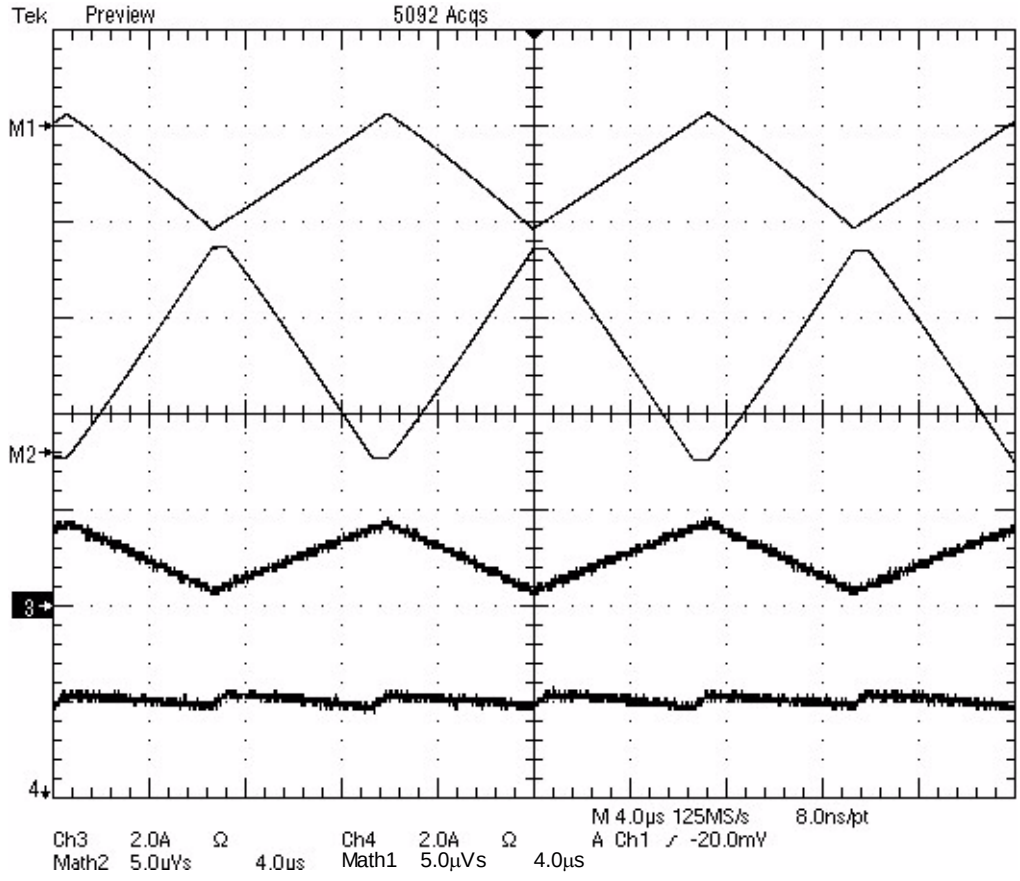

Figure 5.17 AC Flux and Current Waveforms in the Hard-Switched Two-Inductor Boost Converter with Structure A Magnetic Integration

Channel M1: AC Component of Flux ϕ_1 (5 µWb/div),

Channel M2: AC Component of Flux ϕ_c (5 µWb/div),

Channel 3: Current i_1 (2 A/div), Channel 4: Current i_{IN} (2 A/div)

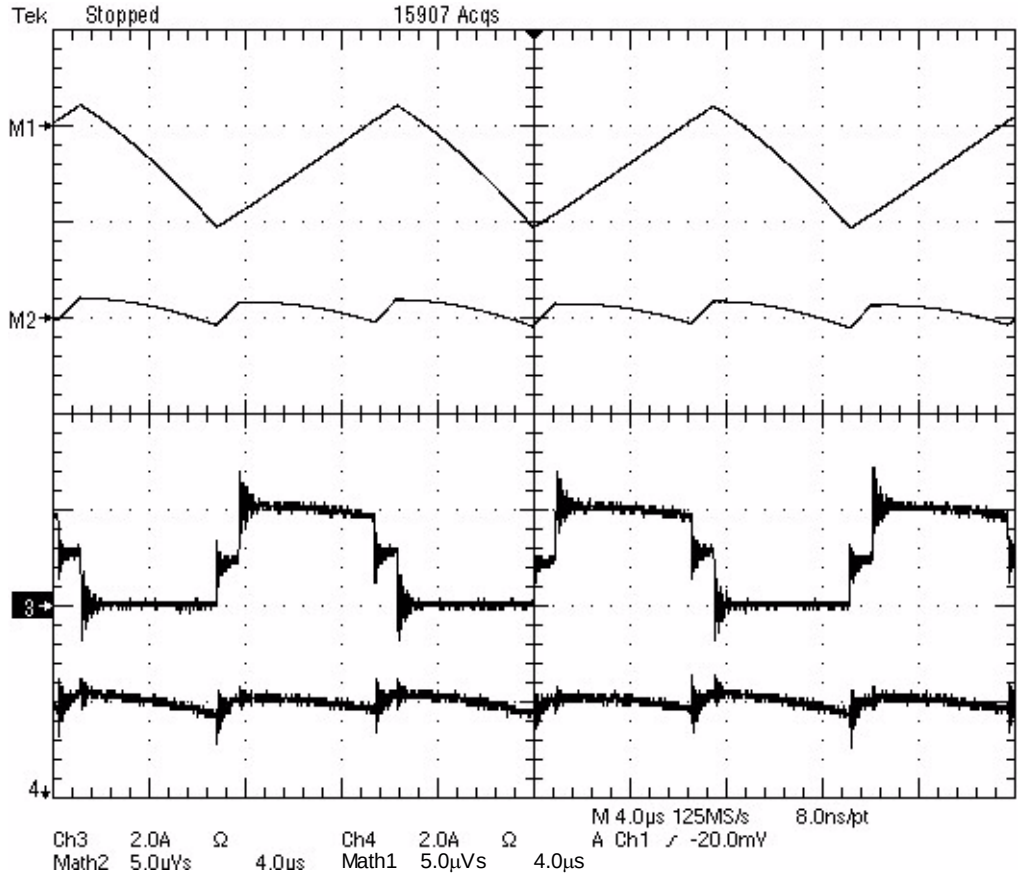

Figure 5.18 AC Flux and Current Waveforms in the Hard-Switched Two-Inductor Boost Converter with Structure C Magnetic Integration

Channel M1: AC Component of Flux ϕ_1 (5 µWb/div),

Channel M2: AC Component of Flux ϕ_c (5 µWb/div),

Channel 3: Current i_1 (2 A/div), Channel 4: Current i_{IN} (2 A/div)

As Structure B has high transformer leakage inductance, it is not suited to the hard-switched converter operation. A soft-switched two-inductor boost converter with Structure B magnetic integration will be introduced in the next section.

5.6 Soft-Switched Two-Inductor Boost Converter with Structure B Magnetic Integration

Amongst the four integrated magnetic structures, Structure B presents the highest transformer leakage inductance as the primary and the secondary windings are located on different core legs. In the operation of the hard-switched two-inductor boost converter, the transformer leakage inductance resonates with the MOSFET output capacitance when the MOSFET turns off and this causes over voltage across the MOSFETs. This adverse effect prohibits the application of Structure B magnetic integration in the hard-switched two-inductor boost converter.

In the ZVS two-inductor boost converter, however, the transformer leakage inductance is actively utilised as part of the resonant inductance and this enables the employment of Structure B magnetic integration in the converter. This section provides a detailed analysis of the application of Structure B magnetic integration in the ZVS two-inductor boost converter with a voltage-doubler rectifier, as shown in Figure 5.19.

5.6.1 ZVS Two-Inductor Boost Converter with Structure B Magnetic Integration

Figure 5.20 shows the proposed ZVS two-inductor boost converter with Structure B magnetic integration.

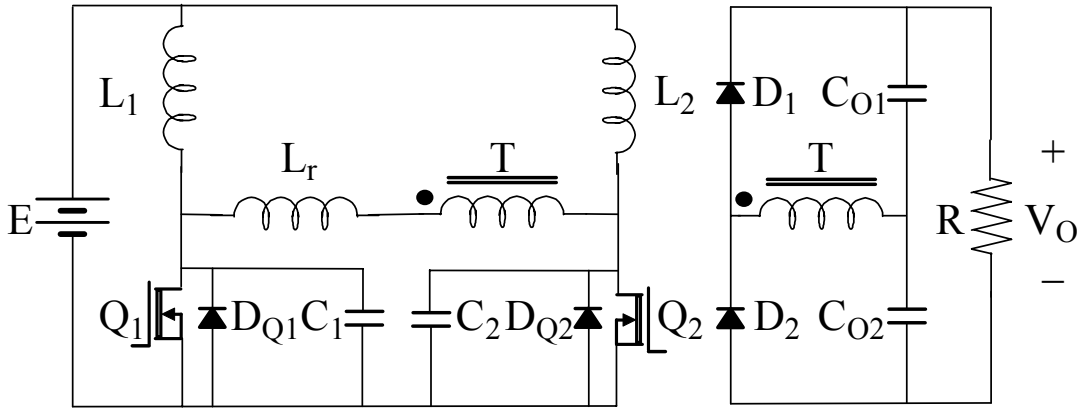

Figure 5.19 ZVS Two-Inductor Boost Converter with a Voltage-Doubler Rectifier

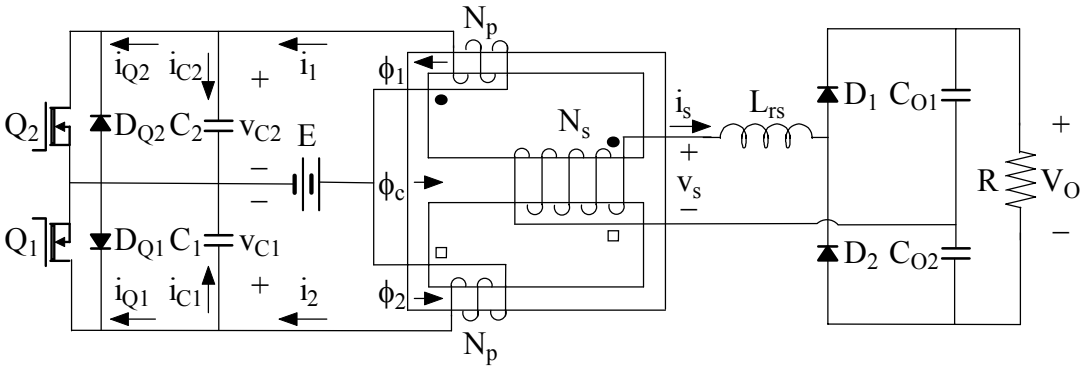

Figure 5.20 ZVS Two-Inductor Boost Converter with Structure B Magnetic Integration

In Figure 5.20, the resonant inductance is placed in series with the transformer secondary winding for the simplicity of the circuit diagram as the transformer primary winding is performed by the two separate windings on the two outer core legs. The resonant inductance in Figure 5.20 can be related to that in Figure 5.19 as:

$$L_{rs} = \frac{N_s^2}{N_p^2} L_r \tag{5.204}$$

The implementation of the resonant inductance normally requires additional high-quality-factor inductors in series with the existing transformer leakage inductance so that the characteristic frequency of the resonant tank is comparable to the converter switching frequency. In Structure B magnetic integration, however, the transformer leakage inductance is much larger than that of the transformer with tight couplings between the primary and the secondary windings and is normally large enough to form the resonant inductance by itself. In this case, the number of magnetic core and copper winding components can be significantly reduced. The four cores and five windings required by the two input inductors, the resonant inductor and the transformer in the ZVS two-inductor boost converter with discrete magnetics are reduced to a single core with three windings. This results in a more compact design with a potentially higher power density.

The resonant capacitances are implemented by the MOSFET output capacitances in parallel with the additional low-dissipation-factor capacitors.

5.6.2 Equivalent Input and Transformer Magnetising Inductances

The equivalent input and magnetising inductances need to be analysed against the soft-switched two-inductor boost converter. The derivatives of the converter instantaneous input and transformer secondary currents in the soft-switched converter with discrete magnetics will be solved first and these will be used as the templates to obtain the equivalent circuit of the soft-switched converter with Structure B magnetic integration. In order to be consistent with the converter

topology in Figure 5.20, the resonant inductor in Figure 5.19 is moved to the transformer secondary side and the converter is redrawn in Figure 5.21.

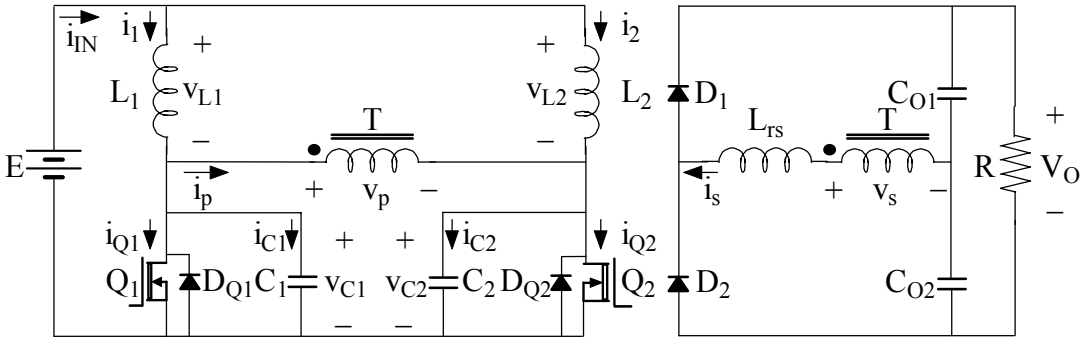

Figure 5.21 ZVS Two-Inductor Boost Converter with the Resonant Inductance in the Transformer Secondary Side

The converter is now analysed under three different operating conditions.

- State (1) ($0 < t < (1 - D_s)T_s$)

  In this state, Q_1 is off while Q_2 is on and $i_{Q1} = 0$. The circuit equations are the same as Equations (5.1) to (5.3) and the derivative of the input current can be obtained as Equation (5.4). The equivalent transformer model in Figure 5.3 can still be used as the transformer leakage inductance is classified as part of the resonant inductance. According to Figure 5.21, the following equations can be obtained:

$$i_p = i_1 - i_{C1} \tag{5.205}$$

$$i_{C1} = C_r \frac{dv_{C1}}{dt} \tag{5.206}$$

$$v_{C1} = v_p \tag{5.207}$$

Manipulations of Equations (5.1), (5.3), (5.5), (5.8), (5.9), (5.205), (5.206) and (5.207) yield:

$$\frac{di_s}{dt} = \frac{N_p}{N_s} \cdot \frac{E}{L} - \left[\frac{1}{L_{ms}} + \left(\frac{N_p}{N_s} \right)^2 \frac{1}{L} \right] v_s - \left(\frac{N_p}{N_s} \right)^2 C_r \frac{d^2 v_s}{dt^2} \tag{5.208}$$

- State (3) $(\frac{T_s}{2} < t < (\frac{3}{2} - D_s)T_s)$

In this state, Q_1 is on while Q_2 is off and $i_{Q2} = 0$. The derivative of the input current can be obtained as Equation (5.14). According to Figure 5.21, the following equations can be obtained:

$$i_p = -i_2 + i_{C2} \tag{5.209}$$

$$i_{C2} = C_r \frac{dv_{C2}}{dt} \tag{5.210}$$

$$v_{C2} = -v_p \tag{5.211}$$

The derivative of the transformer secondary current can then be obtained as:

$$\frac{di_s}{dt} = -\frac{N_p}{N_s} \cdot \frac{E}{L} - \left[\frac{1}{L_{ms}} + \left(\frac{N_p}{N_s} \right)^2 \frac{1}{L} \right] v_s - \left(\frac{N_p}{N_s} \right)^2 C_r \frac{d^2 v_s}{dt^2} \qquad (5.212)$$

- States (2) and (4) ($(1 - D_s)T_s < t < \frac{T_s}{2}$ and $(\frac{3}{2} - D_s)T_s < t < T_s$)

  In these two states, Q_1 and Q_2 are both on. The derivative of the input current can be obtained as Equation (5.11). As the transformer secondary voltage is zero, the derivative of and the transformer secondary current is only determined by the converter output voltage and the resonant inductance and no longer related to the transformer magnetising inductance.

In the hard-switched two-inductor boost converter in Figure 5.9, $i_2 = 0$ in State (1) when Q_1 is off, $i_1 = 0$ in State (3) when Q_2 is off and $i_s = 0$ in States (2) and (4) when Q_1 and Q_2 are both on. Due to the introduction of the resonant capacitors in the soft-switched converter, however, the current in the combined winding is no longer zero when the corresponding MOSFET is off and the current in the transformer secondary winding is no longer a constant zero when both the MOSFETs are on. The magnetic circuit of Structure B is redrawn in Figure 5.22 and this is valid at all times in States (1) to (4).

According to Figure 5.22, the fluxes in the three core legs are respectively:

$$\phi_1 = \frac{N_p i_1}{\Re_o + 2\Re_c}\left(1 + \frac{\Re_c}{\Re_o}\right) - \frac{N_s i_s}{\Re_o + 2\Re_c} + \frac{N_p i_2}{\Re_o + 2\Re_c} \cdot \frac{\Re_c}{\Re_o} \tag{5.213}$$

$$\phi_2 = \frac{N_p i_1}{\Re_o + 2\Re_c} \cdot \frac{\Re_c}{\Re_o} + \frac{N_s i_s}{\Re_o + 2\Re_c} + \frac{N_p i_2}{\Re_o + 2\Re_c}\left(1 + \frac{\Re_c}{\Re_o}\right) \tag{5.214}$$

$$\phi_c = \frac{N_p i_1}{\Re_o + 2\Re_c} - \frac{2N_s i_s}{\Re_o + 2\Re_c} - \frac{N_p i_2}{\Re_o + 2\Re_c} \tag{5.215}$$

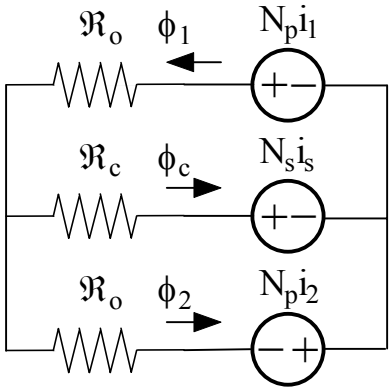

Figure 5.22 Magnetic Circuit of Structure B in the ZVS Two-Inductor Boost Converter

According to Figure 5.20, Equations (5.40) and (5.216) to (5.219) can be obtained.

$$N_p \frac{d\phi_1}{dt} = E - v_{C2} \tag{5.216}$$

$$N_p \frac{d\phi_2}{dt} = E - v_{C1} \tag{5.217}$$

$$i_1 = i_{Q2} + i_{C2} \tag{5.218}$$

$$i_2 = i_{Q1} + i_{C1} \tag{5.219}$$

The converter in Figure 5.20 is now analysed under three different operating conditions.

- State (1) ($0 < t < (1 - D_s)T_s$)

In this state, $v_{C1} > 0$ as Q_1 is off and $v_{C2} = 0$ as Q_2 is on. Equation (5.216) can be rewritten to Equation (5.32). Manipulations of Equations (5.32), (5.40), (5.89) and (5.217) yield:

$$v_{C1} = \frac{N_p}{N_s} v_s \tag{5.220}$$

Substitution of Equation (5.220) to (5.217) yields:

$$N_p \frac{d\phi_2}{dt} = E - \frac{N_p}{N_s} v_s \tag{5.221}$$

As $i_{Q1} = 0$, Equation (5.219) can be rewritten as:

$$i_2 = i_{C1} \tag{5.222}$$

Manipulations of Equations (5.206), (5.220) and (5.222) yield:

$$\frac{di_2}{dt} = \frac{N_p}{N_s} C_r \frac{d^2 v_s}{dt^2} \tag{5.223}$$

Substitution of Equations (5.213), (5.214) and (5.215) to (5.32), (5.40) and (5.221) and manipulations the results with Equation (5.223) yield Equations (5.28) and (5.224):

$$\frac{di_s}{dt} = \frac{N_p}{N_s} \cdot \frac{E}{L_a} - \left[\frac{1}{L_b} + \left(\frac{N_p}{N_s} \right)^2 \frac{1}{2L_a} \right] v_s - \left(\frac{N_p}{N_s} \right)^2 C_r \frac{d^2 v_s}{dt^2} \tag{5.224}$$

- State (3) $(\frac{T_s}{2} < t < (\frac{3}{2} - D_s)T_s)$

In this state, $v_{C1} = 0$ as Q_1 is on and $v_{C2} > 0$ as Q_2 is off. Equation (5.217) can be rewritten to Equation (5.23). Manipulations of Equations (5.23), (5.40), (5.89) and (5.216) yield:

$$v_{C2} = -\frac{N_p}{N_s} v_s \tag{5.225}$$

Substitution of Equation (5.225) to (5.216) yields:

$$N_p \frac{d\phi_1}{dt} = E + \frac{N_p}{N_s} v_s \tag{5.226}$$

As $i_{Q2} = 0$, Equation (5.218) can be rewritten as:

$$i_1 = i_{C2} \tag{5.227}$$

Manipulations of Equations (5.210), (5.225) and (5.227) yield:

$$\frac{di_1}{dt} = -\frac{N_p}{N_s} C_r \frac{d^2 v_s}{dt^2} \tag{5.228}$$

Substitution of Equations (5.213), (5.214) and (5.215) to (5.23), (5.40) and (5.226) and manipulations the results with Equation (5.228) yield Equations (5.36) and (5.229):

$$\frac{di_s}{dt} = -\frac{N_p}{N_s} \cdot \frac{E}{L_a} - \left[\frac{1}{L_b} + \left(\frac{N_p}{N_s} \right)^2 \frac{1}{2L_a} \right] v_s - \left(\frac{N_p}{N_s} \right)^2 C_r \frac{d^2 v_s}{dt^2} \tag{5.229}$$

- States (2) and (4) ($(1 - D_s)T_s < t < \frac{T_s}{2}$ and $(\frac{3}{2} - D_s)T_s < t < T_s$)

In these two states, Q_1 and Q_2 are both on. According to Figure 5.20, Faraday's Law gives Equations (5.23) and (5.32) and Equation (5.41) can be obtained. Manipulations of Equations (5.23), (5.32), (5.40) and (5.89) yield Equation (5.12). Therefore the transformer secondary current is no longer determined by the transformer magnetising inductance.

Comparisons of Equations (5.28), (5.224), (5.36), (5.229) and (5.41) respectively with their discrete magnetic counterparts, Equations (5.4), (5.208), (5.14), (5.212) and (5.11), yield Equations (5.43) and (5.44). Equations (5.43) and (5.44) confirm that the equivalent input and transformer magnetising inductances of Structure B magnetic integration are the inherent characteristics of the magnetic structure and do not change with the hard-switched or the soft-switched two-inductor boost converter topologies.

5.6.3 DC Fluxes

The dc fluxes in Structure B in the ZVS two-inductor boost converter can be analysed in the same process as in the integrated magnetic structures in the hard-switched converter. However, the ac fluxes in the ZVS converter must be established through the state analysis, which will be introduced in the next section.

Assuming that I_1, I_2, I_S are respectively the dc components of i_1, i_2 and i_s over the entire switching period, the following equations can be established as the operation of the ZVS two-inductor boost converter is half cycle symmetrical:

$$I_1 = I_2 = \frac{I_{IN}}{2} \tag{5.230}$$

$$I_S = 0 \tag{5.231}$$

Assuming that $I_{1,j}$, $I_{2,j}$ and $I_{s,j}$ are respectively the dc components of i_1, i_2 and i_s in

State (j), where $j = 1,2,3,4$, the following equation can be established:

$$I_w = \sum_{j=1}^{4} D_j I_{w,j} \ , \ w = 1,2,s \ , \ j = 1,2,3,4 \ , \ D_j = \begin{cases} 1 - D_s , & j = 1,3 \\ D_s - \dfrac{1}{2}, & j = 2,4 \end{cases} \tag{5.232}$$

According to Figure 5.22, the instantaneous fluxes in the three core legs are restricted by Equations (5.51) and (5.233):

$$\Re_o \phi_1 + \Re_c \phi_c = N_p i_1 - N_s i_s \tag{5.233}$$

Equations (5.51) and (5.233) can be respectively rewritten to Equations (5.53) and (5.234) with the dc components of the variables in each state, where Φ_1, Φ_2, Φ_c and I_{IN} are the dc components of ϕ_1, ϕ_2, ϕ_c, i_{IN} in each state and as well over the entire switching period:

$$\Re_o \Phi_1 + \Re_c \Phi_c = N_p I_{1,j} - N_s I_{s,j} , \ j = 1,2,3,4 \tag{5.234}$$

Manipulations of Equations (5.232) and (5.234) yield:

$$\Re_o \Phi_1 + \Re_c \Phi_c = N_p I_1 - N_s I_S \tag{5.235}$$

Substitution of Equations (5.230) and (5.231) to (5.235) yields:

$$\Re_o \Phi_1 + \Re_c \Phi_c = \frac{N_p I_{IN}}{2} \tag{5.236}$$

Equations (5.53) and (5.236) are valid over the entire switching period and the dc fluxes in the individual core legs are the same as those in Structure B in the hard-switched two-inductor boost converter, which are given in Equations (5.61) and (5.62).

5.6.4 State Analysis

As Structure B magnetic integration can be modeled by the discrete magnetics as explained in Section 5.6.2, the operation of the ZVS two-inductor boost converter with integrated magnetics can be analysed based on the converter in Figure 5.19 if the resonant inductance L_{rs} in Figure 5.20 is converted to its equivalent value L_r through Equation (5.204).

After Q_1 turns off, the converter will move through up to four possible states, as shown in Figure 4.4. All symbols have the same physical meanings except that V_d is now the output capacitor C_{O1} or C_{O2} voltage reflected to each of the two combined windings that perform as both the input inductor and the transformer primary. The resonant capacitor voltage and the inductor current are the same as those presented in Section 4.3.1 and the flux in one outer core leg will be analysed here.

- State (a) ($0 \le t \le t_1$)

While v_{C1} increases in this state, ϕ_2 increases but with a reducing rate as long as $v_{C1} < E$. When $v_{C1} > E$, ϕ_2 decreases with an increasing rate. If the initial flux $\phi_2(0) = \Phi_{20}$, the flux ϕ_2 is:

$$\phi_2(t) = \frac{(E + V_d)\omega_0 t + (1 + \Delta_1) I_0 Z_0 (\cos \omega_0 t - 1) - V_d \sin \omega_0 t}{\omega_0 N_p} + \Phi_{20} \qquad (5.237)$$

The derivation of Φ_{20} will be given in due course after the state analysis is completed.

- State (b) ($t_1 \le t \le t_2$)

In this state, the flux ϕ_2 encounters the same situation as in State (a). The flux ϕ_2 is:

$$\phi_2(t) = \frac{\left[E - v_{C1}(t_1)\right](t - t_1) - \frac{I_0}{2C_1}(t - t_1)^2}{N_p} + \phi_2(t_1) \qquad (5.238)$$

- State (c) ($t_2 \le t \le t_3$)

In this state, the flux ϕ_2 keeps decreasing with an increasing rate until v_{C1} reaches its peak and continues to decrease as long as $v_{C1} > E$. After v_{C1} falls

below E, ϕ_2 again increases at an increasing rate. The flux ϕ_2 is:

$$\phi_2(t) = \frac{(E - V_d)\omega_0(t - t_2) + I_0 Z_0\left[\cos\omega_0(t - t_2) - 1\right]}{\omega_0 N_p} - \frac{\left[v_{C1}(t_2) - V_d\right]\sin\omega_0(t - t_2)}{\omega_0 N_p} + \phi_2(t_2) \tag{5.239}$$

- State (d) ($t_3 \le t \le t_4$)

In this state, the flux ϕ_2 increases linearly as the capacitor voltage v_{C1} is zero. The flux ϕ_2 is:

$$\phi_2(t) = \frac{E(t - t_3)}{N_p} + \phi_2(t_3) \tag{5.240}$$

According to the above state analysis, the flux ϕ_2 reaches its maximum $\phi_{2,max}$ when the capacitor voltage v_{C1} first reaches E in either States (a) or (b) and reaches its minimum $\phi_{2,min}$ when the capacitor voltage v_{C1} drops back to E in State (c). The ac fluxes in the outer core legs $|\Delta\phi_1|$ and $|\Delta\phi_2|$ can be calculated by integrating Equation (5.217) between the times when the flux ϕ_2 reaches $\phi_{2,max}$ and $\phi_{2,min}$. Therefore, the peak flux $\phi_{2,max}$ can be obtained as:

$$\phi_{2,\max} = \Phi_2 + \frac{|\Delta\phi_2|}{2} \tag{5.241}$$

The initial flux Φ_{20} can then be derived by subtracting the flux increase between the instant when Q_1 turns off and the instant when v_{C1} first reaches E from the peak flux $\phi_{2,max}$.

The flux ϕ_1 in the other outer core leg can be analysed in the same way. Under symmetrical operation, the flux waveforms of the two outer core legs are the same except that they are phase shifted with 180°.

Because the transformer primary and secondary windings are loosely coupled in Figure 5.20, the resonant inductance can be purely realised from the transformer leakage inductance. In this case, the leakage flux in the transformer is significant and the flux paths are not constrained within the core structure. Considering the leakage flux, Structure B magnetic circuit shown in Figure 5.22 can be redrawn in Figure 5.23, where $\Re_a$ is the reluctance of the transformer leakage flux path in the air and ϕ_{le} is the transformer leakage flux, which has the same direction as the flux in the centre core leg.

The flux in the centre core leg and the leakage flux are respectively:

$$\phi_c = \phi_1 - \phi_2 - \phi_{le} \tag{5.242}$$

$$\phi_{le} = \frac{L_{rs} i_s}{N_s} \tag{5.243}$$

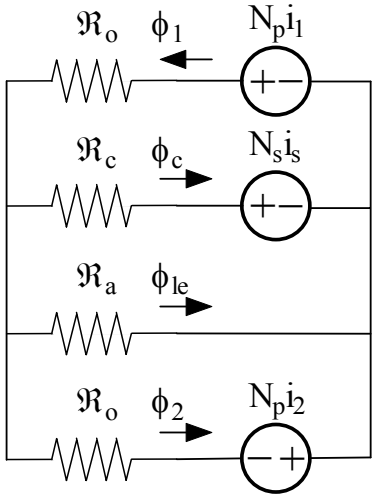

Figure 5.23 Structure B Magnetic Circuit with the Leakage Flux Path

It is worth mentioning that Equation (5.40) can also be used to solve the flux in the centre core leg. As the resonant inductance is made up of the transformer leakage inductance, v_s in Equation (5.40) is the positive voltage across the capacitor C_{O1} or the negative voltage across the capacitor C_{O2} in the voltage-doubler rectifier. When the transformer secondary current is positive, $v_s > 0$ and ϕ_c linearly increases and when the transformer secondary current is negative, $v_s < 0$ and ϕ_c linearly decreases.

5.6.5 Theoretical and Experimental Waveforms

The proposed topology is validated experimentally by a 40-W converter with 20-V input. A conversion efficiency of 93% has been recorded by using the mathematics functions of a Tektronix TDS5034 oscilloscope equipped with the input and output voltage and current probes. The components used in the converter are listed below:

- Inductors L_1 and L_2 and Transformer T – Core type Philips ETD29 with a 0.5-mm air gap in each of the two outer core legs, minimum centre core leg cross section area 71 mm^2 [167], ferrite grade Philips 3F3, Structure B magnetic integration, primary and secondary wires: Litz wires made up of 50 strands of 0.11-mm (0.135-mm overall diameter) wire, primary winding $N_p = 10$ turns, secondary winding $N_s = 13$ turns, leakage inductance reflected to the transformer secondary $L_{les} = 12.39\ \mu H$.
- Additional Resonant Capacitors – Cornell Dubilier surface mount mica capacitor MC22FA202J, 2 nF, $V_{dc} = 100\ V$, $DF = 1/6000$ at 500 kHz, 6 nF capacitance used.
- MOSFETs Q_1 and Q_2 – ST STB50NE10, $V_{DS} = 100\,V$, $I_D = 50\ A$, $R_{DS(on)} = 0.027\ \Omega$, $C_{oss} = 0.675\ nF$.
- Diodes D_1 and D_2 – Motorola MBRS1100T3 surface mount diodes, $V_{RRM} = 100\,V$, $I_F = 1.0\ A$, $V_F = 0.75\,V$.
- Capacitors C_{O1} and C_{O2} – AVX surface mount capacitors 0.47 μF, $V_{dc} = 50\,V$.

The other parameters used in the converter design are listed below:

- The switching frequency $f_s = 500\ kHz$ and the duty ratio $D_s = 0.60$.
- $k = 1.4$, $\Delta_1 = 1.9$ and $V_d / E = 1.15$.
- $L_r = 7.33\ \mu H$ and $C_r = 6.65\ nF$.

The theoretical waveforms of the MOSFET gate voltage, the resonant capacitor voltage, the resonant inductor or the transformer secondary current and the fluxes in the two outer and the centre core legs under the above operating conditions are given in Figure 5.24.

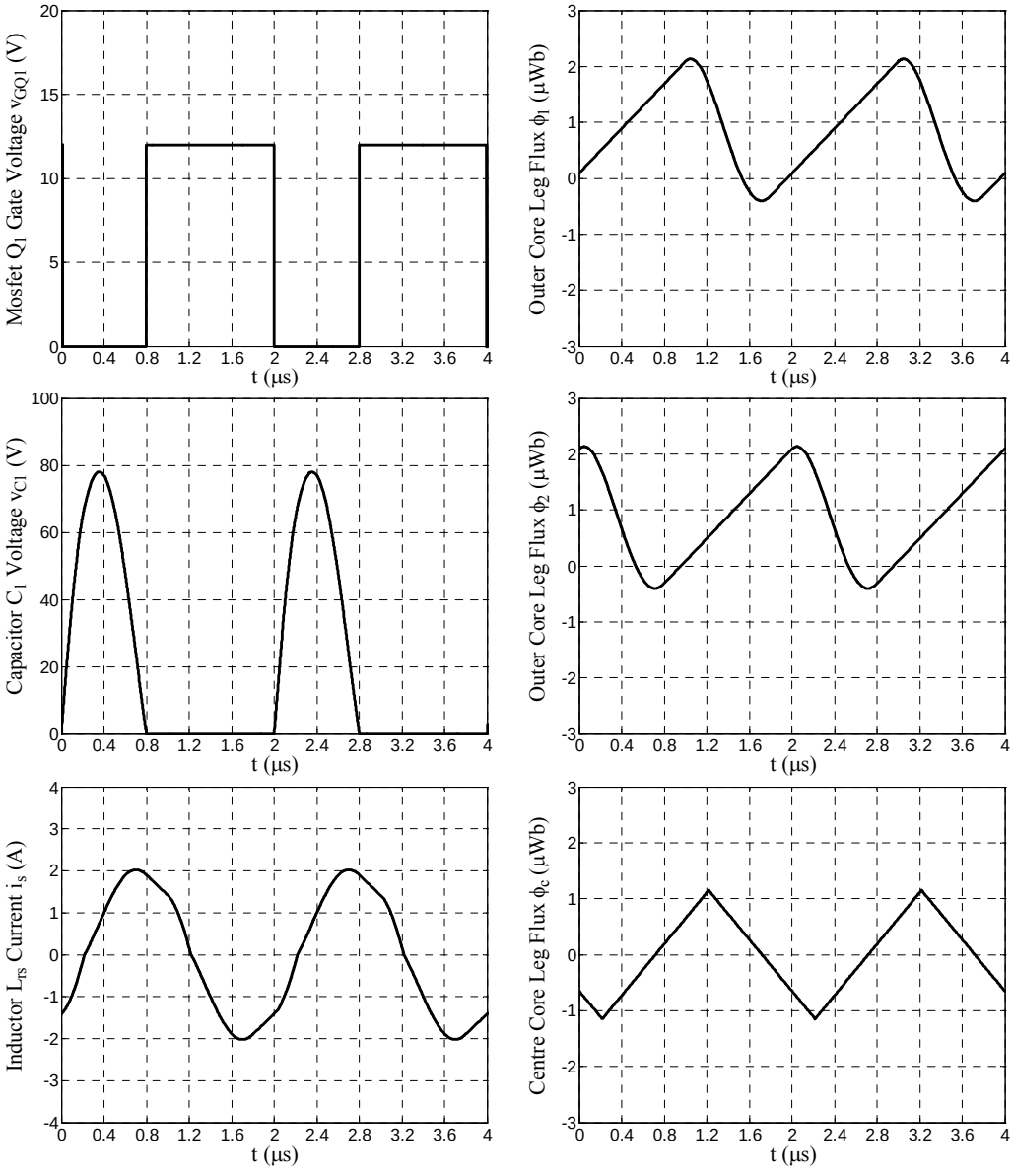

Figure 5.24 Theoretical Waveforms

Under the above operating conditions, the dc flux is 0.87 μWb and the ac flux is 2.54 μWb peak to peak in the two outer core legs. The peak flux density in the outer core leg is 60 mT. The ac flux is 2.30 μWb peak to peak and the peak flux density is 16 mT in the centre core leg.

The experimental waveforms are shown in Figures 5.25 and 5.26. From top to bottom, Figure 5.25 shows the MOSFET gate voltage, the resonant capacitor voltage and the transformer secondary current.

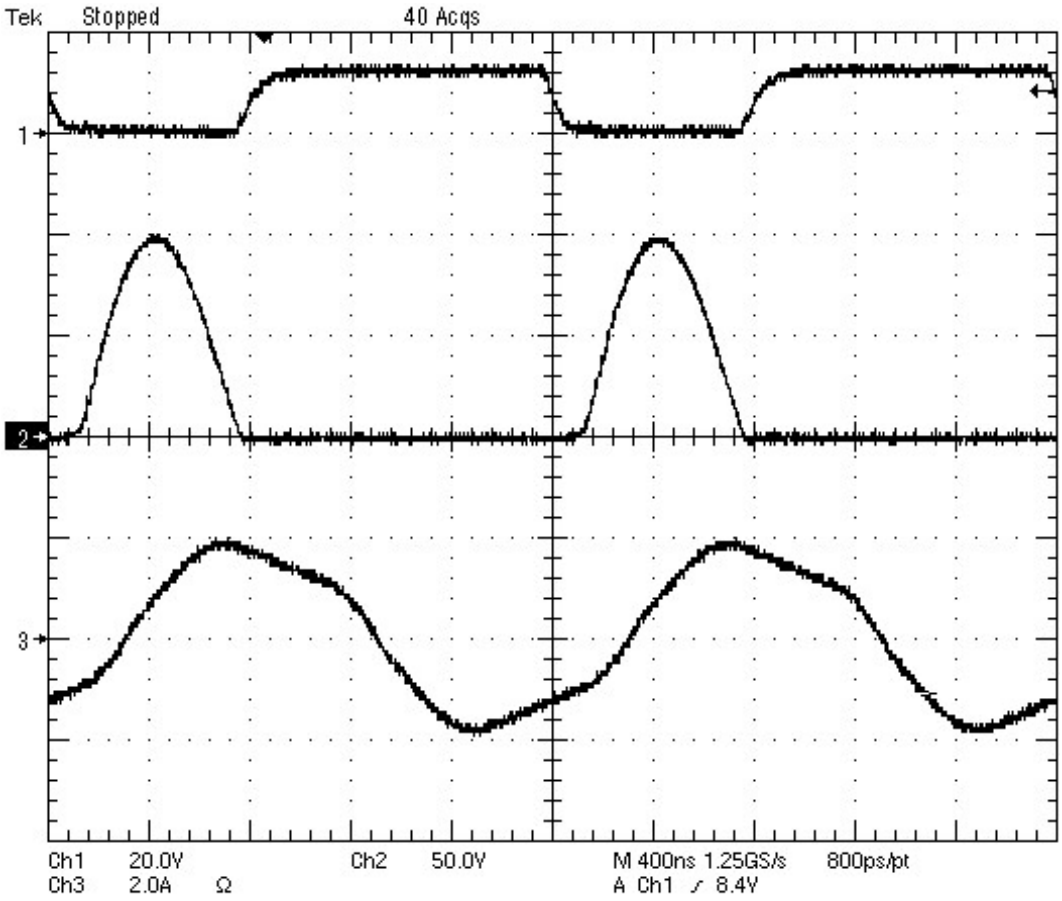

Figure 5.25 Experimental Voltage and Current Waveforms

The top two waveforms in Figure 5.26 are respectively the ac flux waveforms of ϕ_2 and ϕ_c as recovered by integrating the voltage of a single search turn wound on the transformer core leg. The bottom two waveforms are respectively the resonant capacitor voltage v_{C1} and resonant inductor current i_s and they are repeated here as the references for the flux waveforms.

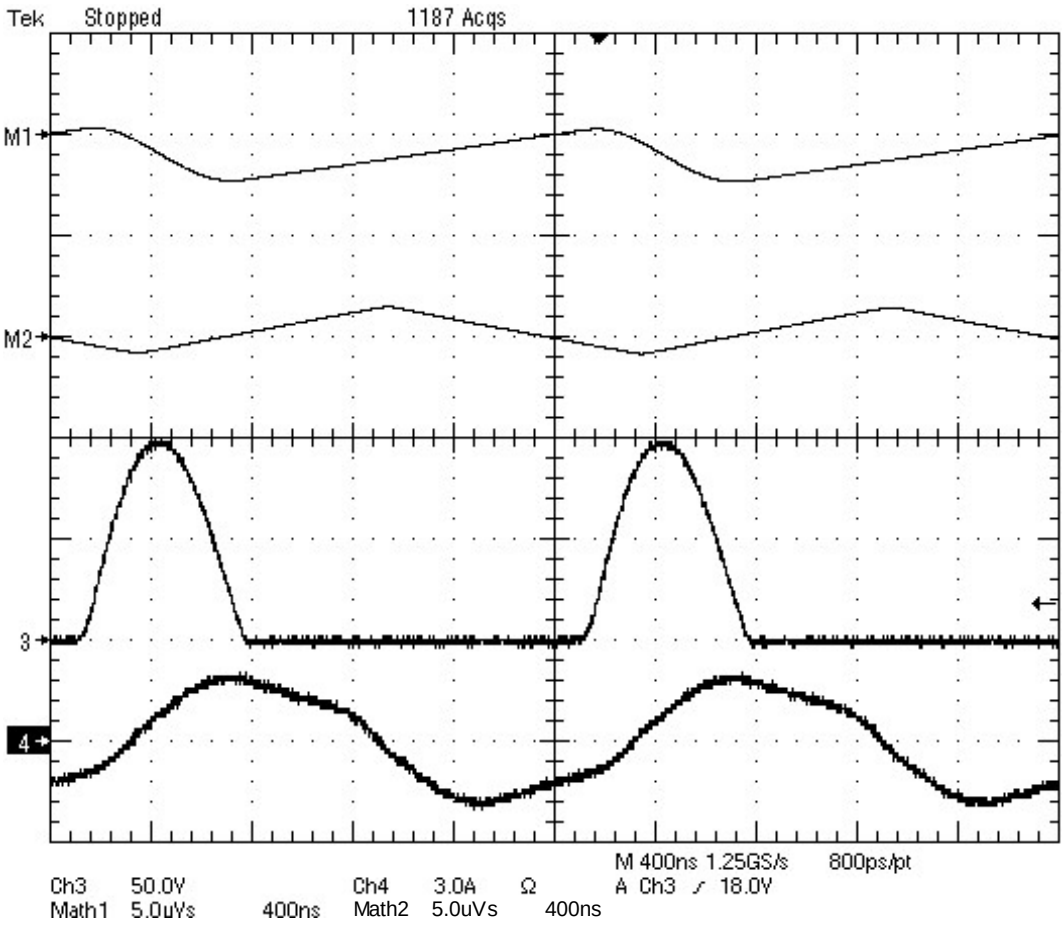

Figure 5.26 Experimental AC Flux, Voltage and Current Waveforms

Channel M1: AC Component of Flux ϕ_2 (5 μWb/div),

Channel M2: AC Component of Flux ϕ_c (5 μWb/div),

Channel 3: Voltage v_{C1} (50 V/div), Channel 4: Current i_s (3 A/div)

It can be observed in Figure 5.26 that the flux ϕ_2 decreases when $v_{C1} > E$ and increases when $v_{C1} < E$. The flux ϕ_c linearly increases when $i_s > 0$ and linearly decreases when $i_s < 0$. The experimental waveforms in Figures 5.25 and 5.26 agree very well with the theoretical waveforms in Figure 5.24.

5.7 Summary

This chapter systematically studies four magnetic integration solutions for the two-inductor boost converter, which are able to integrate the core and the winding components required by separate magnetic devices and lead to the converter design with the minimised size and cost. In the converter with magnetic integration, the equivalent input and transformer magnetising inductances, the dc gain, the dc and ac flux densities in the individual core legs and the current ripples in the individual windings are thoroughly investigated. The theoretical waveforms are provided for the hard-switched two-inductor boost converter with each of the four integrated magnetic structures and the experimental waveforms are provided for the hard-switched two-inductor boost converter with Structures A and C magnetic integration. The ZVS two-inductor boost converter with Structure B magnetic integration is also studied in detail and both the theoretical and the experimental waveforms are provided for a prototype 40-W converter.